ICE LOADS ON PROPELLERS UNDER EXTREME OPERATING CONDITIONS

GOTTUMUKKALA CHANDRASEKHAR VARMA

INFORMATION TO USERS

This manuscript has been reproduced from the microfilm master. UMI films the text directly from the original or copy submitted. Thus, some thesis and dissertation copies are in typewriter face, while others may be from any type of computer printer.

The quality of this reproduction is dependent upon the quality of the copy submitted. Broken or indistinct print, colored or poor quality illustrations and photographs, print bleedthrough, substandard margins, and improper alignment can adversely affect reproduction.

In the unlikely event that the author did not send UMI a complete manuscript and there are missing pages, these will be noted. Also, if unauthorized copyright material had to be removed, a note will indicate the deletion.

Oversize materials (e.g., maps, drawings, charts) are reproduced by sectioning the original, beginning at the upper left-hand corner and continuing from left to right in equal sections with small overlaps.

Photographs included in the original manuscript have been reproduced xerographically in this copy. Higher quality 6" x 9" black and white photographic prints are available for any photographs or illustrations appearing in this copy for an additional charge. Contact UMI directly to order.

ProQuest Information and Learning
300 North Zeeb Road, Ann Arbor, MI 48106-1346 USA
800-521-0600

Ice Loads on Propellers Under Extreme Operating Conditions

By
©Gottumukkala Chandrasekhar Varma, B.Eng.

A thesis Submitted to the school of Graduate Studies
in Partial Fulfilment of the
Requirements for the Degree of
Master of Engineering

Faculty of Engineering and Applied Science
Memorial University of Newfoundland
August, 2000

St.John's **Newfoundland** **Canada**

Abstract

The research focus is on ice-class propellers. Methods exist for predicting hydrodynamic and contact ice loads on conventional ice-class propellers under normal operating conditions in ice. These have been used to develop a preliminary design and analysis procedure for propeller blade strength. The present research aims to extend these ice load predictions to extreme and transient operating conditions.

To address these extreme conditions, a numerical model was developed using existing empirical results of ice-structure interaction. This model was incorporated into an existing Fortran code for predicting ice loads on propellers under normal operating conditions. The refined code was used to predict loads on a series of propellers under extreme operating conditions such as when the propeller was stopped and the ship is moving and these results were used to check the design procedure.

To verify the correctness of the numerical model a series of model scale indentation tests were performed at the Institute of Marine Dynamics, using an MTS machine. A propeller blade shaped indentor with a geometry of that of *R-Class* propeller was used as an indentor to indent against laboratory grown ice. The tests were performed at high speeds. These results are compared with the numerical simulations.

Acknowledgements

I express my sincere gratitude to Dr. Brian Veitch and Dr. Neil Bose for their guidance, financial support and advice. They were always there to guide me in proper direction whenever I made a mistake, right from the initial days through the completion of this thesis. They taught me new methods to deal with problems.

I wish to extend my special thanks to Dr. Stephen Jones, Brian Hill and Austin Bugden of Institute of Marine Dynamics for their advice and assistance during my experimental process. I wish to convey special thanks to Andrew Fisher of Memorial University for his valuable assistance in the manufacture of the indentor. Thanks are extended to the staff of Tech. Services at MUN, for their help in manufacture of the testing equipment.

I wish to convey my special thanks to my parents and my brother for allowing me to come to Canada for higher studies and their moral support. Thanks to my family and friends for their moral support.

Table of Contents

List of Figures

Chapter 1

Introduction

1.1 Aim

The subject of research reported in the present work is the loading phenomenon that occurs when marine screw propellers interact with sea ice. The primary concern of this work was the propeller-ice contact process that gives rise to extreme loads on propellers' blades. The events of interest were those that result in ice contact loads that act substantially to bend a propeller blade in its weakest direction.

Such events can occur, for example, during icebreaker ramming cycles when the ship changes from ahead to astern motion. For some relatively short time the propeller shaft can be stopped while the ship has forward way. Under these circumstances collision with submerged sea ice can result in the blades' indentation of the ice. The geometry of the indentation is such that the ice fails on the propeller blade's suction side and the loads tend to bend the blade backwards. If the ice is relatively small, the load will be limited by momentum, but if it is large or its motion constrained, the load will be the indentation, or penetration load. Propeller blades can be and have, been bent or broken by this type of event. How frequently this occurs is difficult to gauge, but the fact that there has been for some time a regulatory requirement in the Russian Arctic for icebreaking vessels to have the means to replace broken blades while at sea suggests that it is not rare.

This operational scenario, which has been referred to, perhaps inaccurately, as an off design condition, is not the only one that can result in blade loss due to extreme ice loads. Similar blade loading can also occur during manoeuvring in ice, which is often done aggressively in difficult ice conditions. The recent introduction of azimuthing propellers on ice-going ships adds another dimension to the propeller-ice contact problem.

The aim of the present work is to develop a model of the ice loads on propeller blades that is capable of predicting the loads during indentation of ice such as might occur in the circumstances described above.

1.2 Scope and Approach

An idealized version of the indentation contact is illustrated in Figure 1 in terms of propeller kinematics for a fixed pitch propeller. The figure shows an expanded blade section with a local pitch angle ϕ and the idealized contact geometry associated with different combinations of tangential and axial advance velocities. Under normal steady state forward operations, the combination of tangential and axial velocities means that the section's angle of attack α is positive and quite small. Contact with ice in this situation is concentrated near the blade's leading edge and results in ice milling, as shown in the photograph in Figure 2. A load prediction model of propeller-ice milling has been reported by Veitch (1995), but is not capable of dealing with cases where the angle of attack is negative.

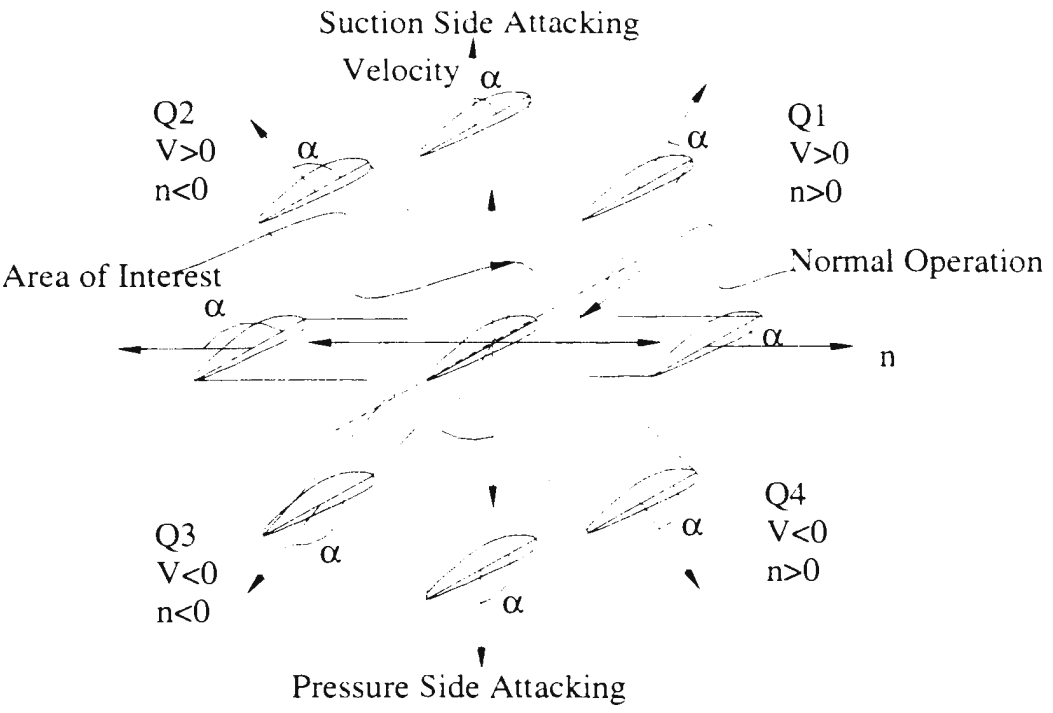

Figure 1. Blade section kinematics and idealized ice contact geometry.

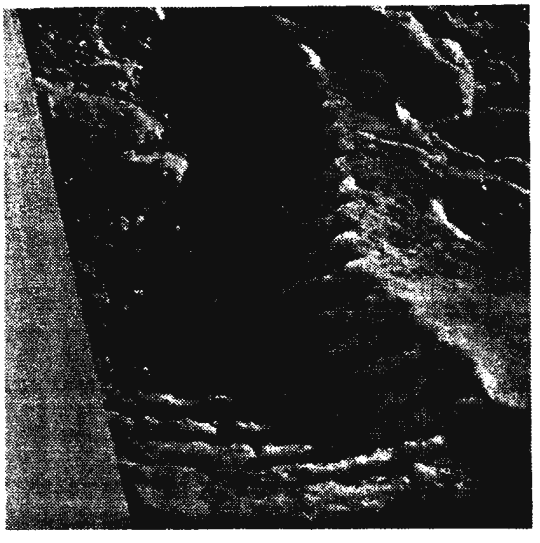

Figure 2. Photograph of milled ice block (Courtesy of C. Daley).

At negative angles of attack, the dominant ice failure mechanism is crushing on the blade's suction side, which is different from the combined crushing and spalling that occurs during milling at positive angles of attack. In the worst case, the tangential velocity is zero and the forward speed is non-zero, which results in indentation contact and penetration. During transient operations when the propeller shaft is rotating slowly while the ship is moving, or when an azimuthing propeller is rotating about a vertical axis, the situation can approach the worst case.

This thesis is concerned with contact loads that occur at negative angles of attack, particularly those at large angles, up to and including the worst case, as indicated in Figure 1. Note that while this discussion so far has been in the context of forward operations, the work applies equally to the corresponding reverse operations and to controllable pitch propellers, the latter illustrated in Figure 3. For fixed pitch propellers, these loads are the maxima that occur in quadrants 1 and 3, that is, when the shaft speed n and advance speed are both greater than zero, and shaft speed and advance speed are both less than zero, respectively. These situations correspond to advance coefficients that are very large and approach infinity.

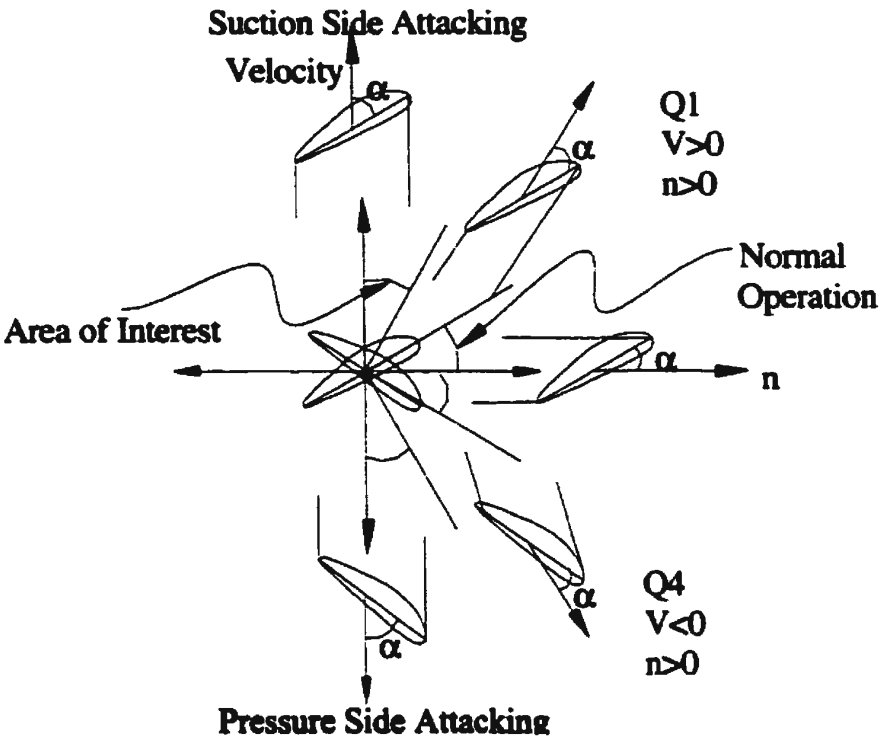

Figure 3. Section kinematics and ice contact geometry for controllable pitch propeller.

Experimental work reported by Searle et al. (1999) investigated ice loads on a propeller at model scale in all operating quadrants, including tests at high advance coefficients that resulted in load reversals. Tests at even higher advance coefficients were not done because of the risk of damaging the model propeller and instrumentation. Some of those results are presented in Figure 4. The extreme load model developed here complements Searle et al.'s experimental results by establishing the maximum reversed loads, indicated schematically in Figure 4.

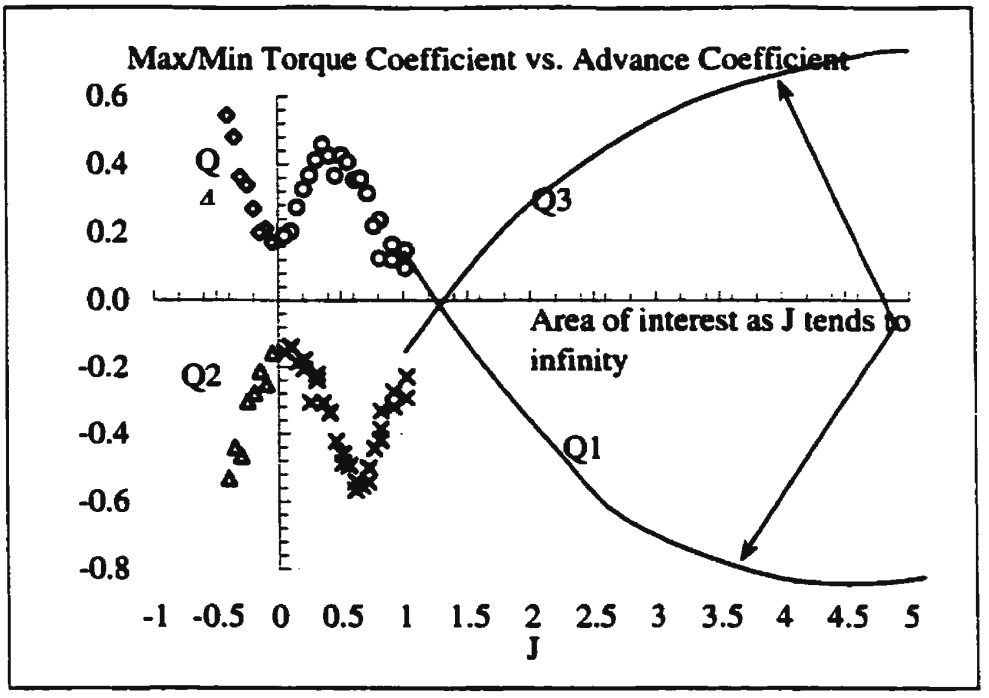

Figure 4. Propeller load coefficients in 4 quadrants (Searle et al. 1999)

The extreme load contact model is based on a statistical analysis of empirical data on ice-structure contact loads. The data was taken from various model scale and medium scale experiments conducted in the Canadian Arctic. The model is presented in Chapter 2 and includes a review of the relevant literature.

The model is applied in Chapter 3 using the *R-Class* propeller blade geometry as an indentor. Cases of indentation with finite ice pieces are also considered, in order to investigate how loads might be limited in practice. Loads are evaluated using a modified version of the propeller-ice interaction simulation code developed by Veitch (1995).

Laboratory experiments of small-scale ice indentation, which were done to test the validity of the load model, are described in Chapter 4, along with the results.

In Chapter 5, the model predictions and lab results are compared and the comparison discussed. Extreme loads are then predicted for several propeller and these are compared with the extreme load model used by Bose *et al.* (1998) in their ice-class propeller design approach.

The conclusions drawn from the work are presented in Chapter 6.

Chapter 2

Model of Blade-Ice Contact Loads

2.1 Review of work on propeller-ice interaction

Jussila and Soininen (1991) and Veitch (1991) carried out two extensive literature reviews in the field of propeller-ice interaction. These reviews discussed in detail the work done by Jagodkin (1963), Ignatjev (1964, 1966), Gabel *et al.* (1979), Belyashov and Shapakov (1983), Wind (1983), Kotras *et al.* (1985). and Chernuka *et al.* (1989). These reviews also presented an extensive review of experimental work carried out. Laboratory tests in this field have been reported by Enkvist and Johansson (1968), Okamoto et al. (1981), Sasajima *et al.* (1981), Sasajima and Mustamaki (1984), Sasajima (1985), Bulat *et al.* (1985), Lindroos and Bjorkestam (1986), Keinonen and Browne (1990), and Jussila and Soninen (1991). Full-scale tests were described in detail by Duff *et al.* (1985), Koskikivi and Kujala (1985), Kannari (1988), Jussila (1983), and Jussila and Koskinen (1989a, 1989b, 1991).

Searle (1999) carried out an extensive review of the recent work done on ice-propeller interaction. He gave a detailed description of the work done by Browne (1990), Browne *et al.* (1991a, 1991b), Newbury *et al.* (1993, 1994), Tamura *et al.* (1997), Belyashov (1993), Veitch and Kivela (1993), Soininen *et al.* (1995), Shih and Zheng (1992, 1993), Yamaguchi (1993), Bose (1996), Liu (1996), Walker *et al.* (1994a, 1994b, 1994c and 1996), Soininen *et al.* (1997), Katzmann and Andriushin (1997) and Bose *et al.* (1998).

Edwards (1976) conducted a series of model-scale milling experiments to address the critical ice breaking issues ignored by Jagodkin (1963), such as backing and ramming. The tests were of two different types: Indentation tests with zero rotational speed and milling tests when the propeller is rotating. The tests used a plastic/wax synthetic ice. He concluded that the blade bending moments varied sinusoidally with the angle of incidence. He also concluded that the main parameters affecting the ice loads on propellers are angle of attack, depth of cut, ice strength and pitch angle.

All the methods cited above focused on conventional propellers. To address the issues of unconventional propellers and operation in four quadrants, a model test program was carried out by Searle (1999). He used two types of propellers in his test program. He conducted tests in all four quadrants of propeller operation and concluded that the propeller loads due to ice strongly depend on the propeller operating conditions. Propellers experience the most extreme loads when a stopped propeller interacts with ice pieces. The present thesis focuses on this issue.

2.2 Statistical Analysis

2.2.1 Pressure – Area Relationship

There are few published full-scale data concerning propeller-ice milling interaction and none on propeller-ice indentation. Several laboratory experiments investigated the contact and indentation of ice by propeller blades (Belyashsov and Shpakov 1983, Veitch 1994, Soininen et al. 1995), although these were all done with relatively small contact areas. The approach taken to formulate the ice-propeller indentation model is based on the existing results of ice-structure indentation. For most of the data collected for ice-structure indentation problem, the parameters measured were contact area and contact pressure. Every dataset used in the analysis has a contact area, so the approach of pressure-area is taken to formulate the ice-propeller indentation model.

Contact area plays a very important role in the contact pressures on structures due to ice loading. To study the problem of ice loads on propeller blades, a relationship between the pressure and area was formulated using the existing results of various small and medium scale experiments. The data sets in analyzing the pressure-area relationship were chosen such that the contact area resembles closely to contact areas of propeller-ice contact (ideally $< 2\ m^2$).

Daley (1994) presented a compilation of medium-scale ice indentation tests that have been conducted in the Canadian Arctic. The work was initiated in 1984 when a group of oil companies conducted indentation tests with iceberg ice at Pond Inlet. In 1989 and

1990, under the supervision of Canadian Coast Guard and National Research Council of Canada, more tests were carried out to investigate ice loads on ships. Medium-scale indentation tests were carried out at Hobson's Choice Ice Island. Various types of indentors were used in these tests. The main interest of these tests was to investigate the ice failure process. In 1993 a series of flaking tests were conducted at Resolute.

The main feature of the above test results was a comparison of ice-pressure and contact area. The data from the above compilation where the contact area was less than 2 m^2 (approximate contact area in actual propeller-ice collisions) has been analyzed. Each data set was analyzed separately, since the tests were performed under different operating conditions. The data sets have a lot of variability (different contact pressures for the same contact area, which may be due to experimental errors or natural phenomenon of ice failure). The variability in the datasets was reduced by taking the average of the maximum pressures for the same contact area. The ice pressure was then plotted against contact area and an exponential curve is fitted to the data.

All the data sets were plotted in a similar fashion and an exponential curve was fitted to each. The equation of the power line is of the form

$$P = C_1 A^{-C_2} \qquad (1)$$

where, P is the Pressure (MPa), A is the Area of contact (m^2), C_1 and C_2 are constants. A total of eight data sets were analyzed in this fashion and each data set produced different values for C_1 and C_2. The plots are presented in Figures 5 through 12.

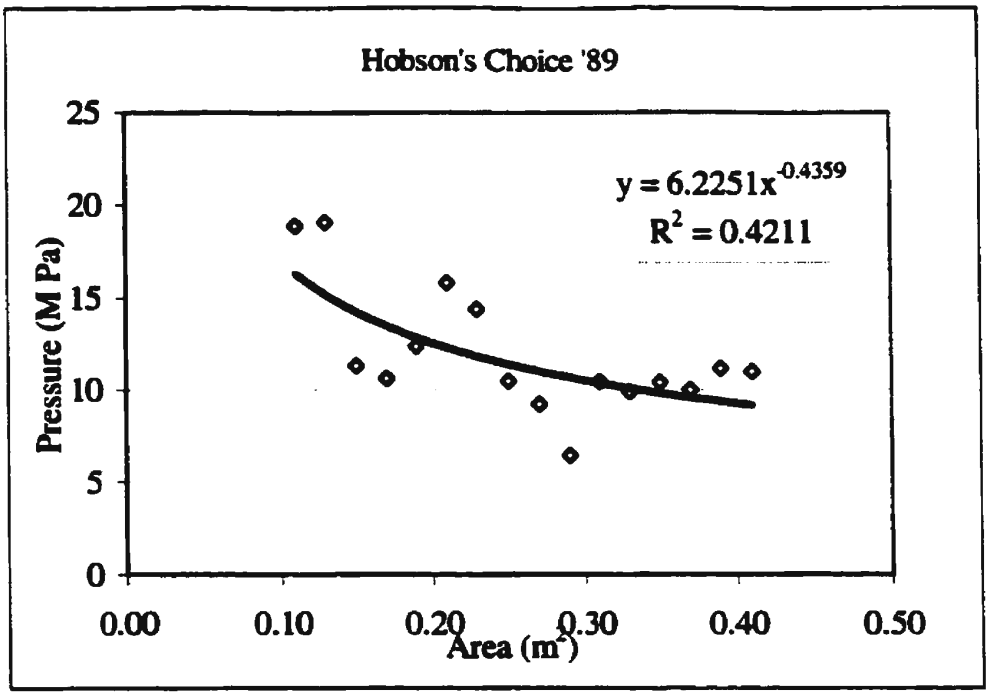

Figure 5. Hobson's Choice '89

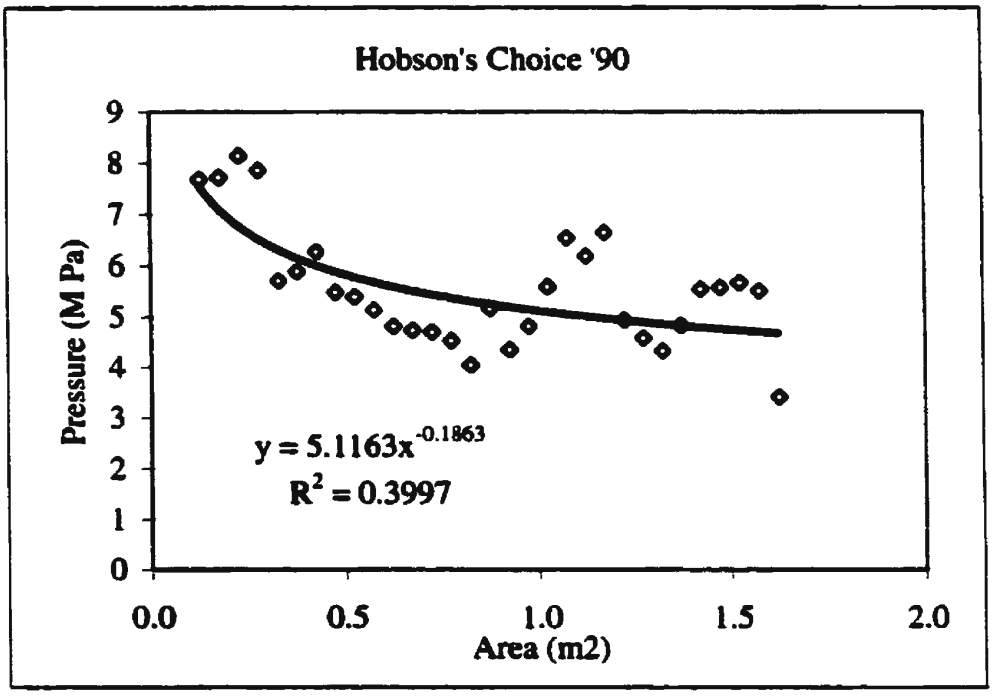

Figure 6. Hobson's Choice '90

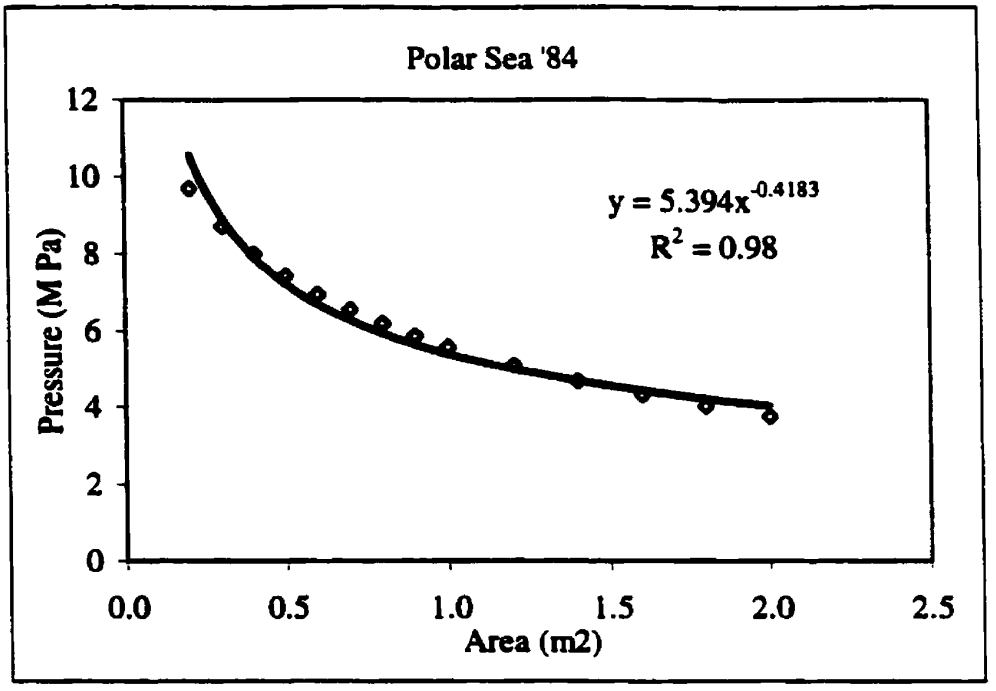

Figure 7. Polar Sea '84

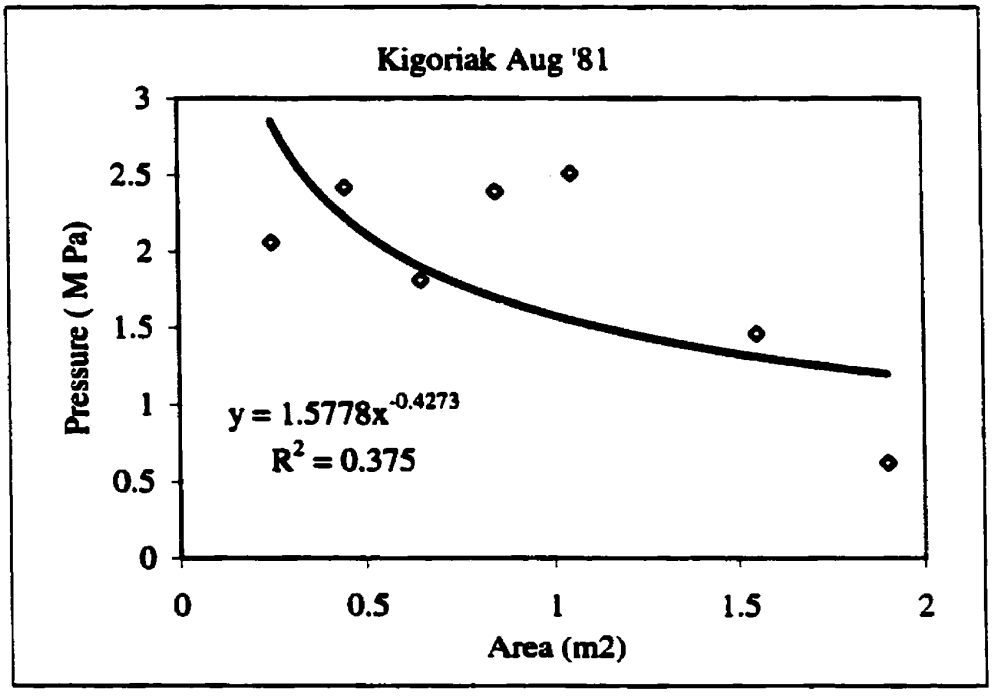

Figure 8. Kigoriak Aug '81

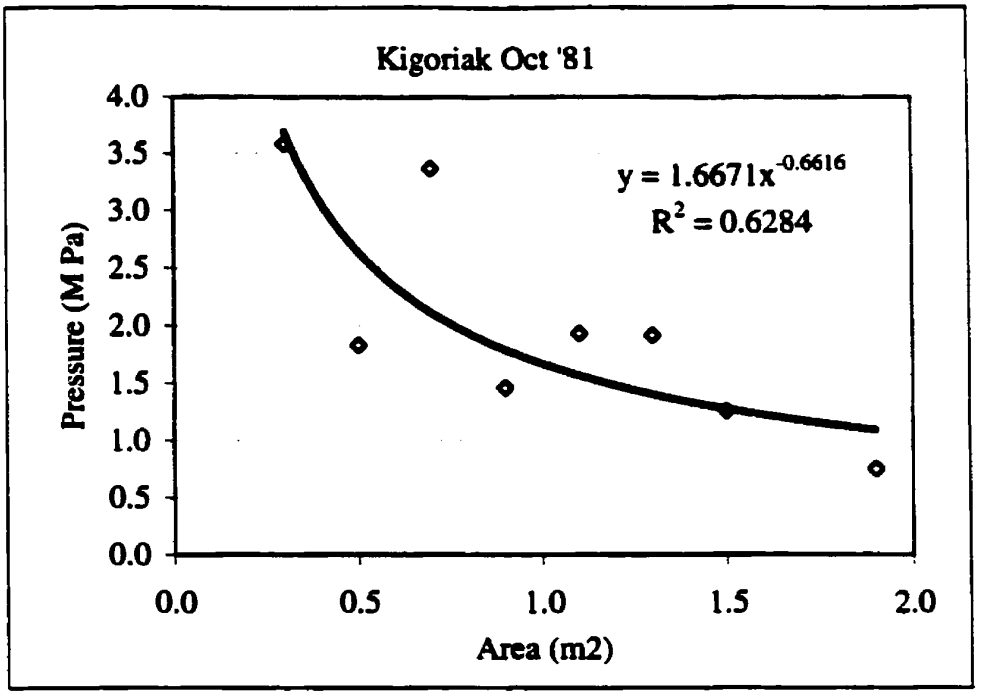

Figure 9. Kigoriak Oct '81

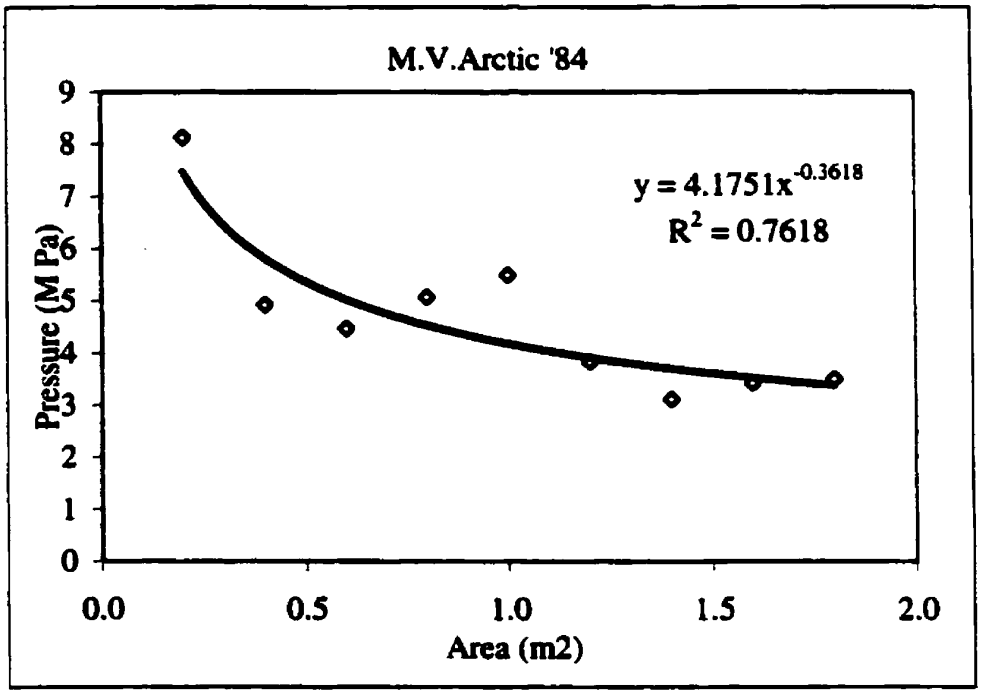

Figure 10. M.V Arctic '84

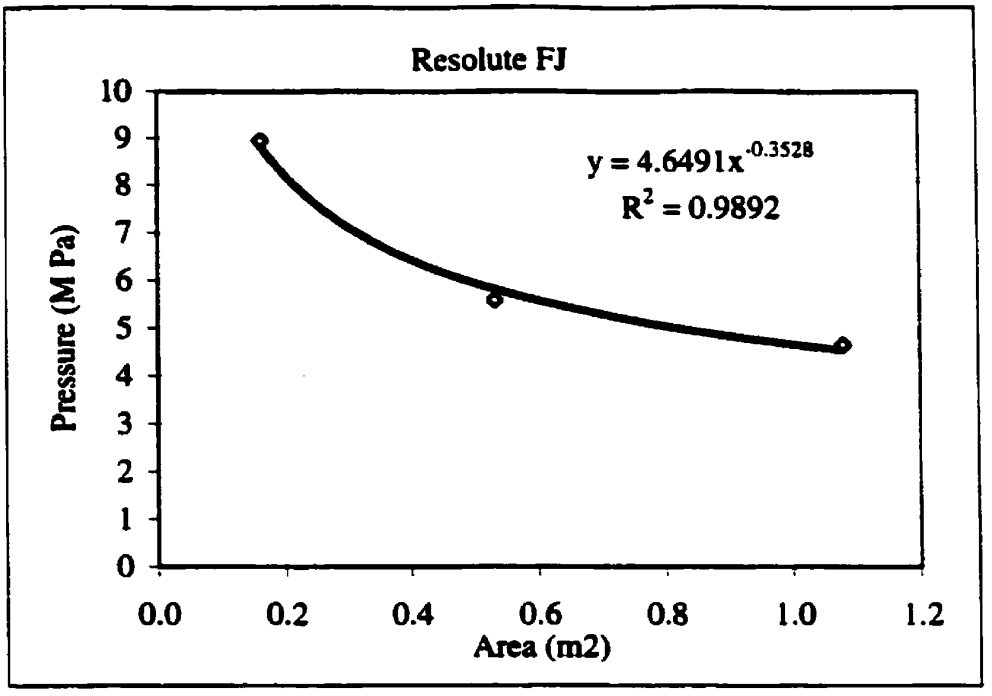

Figure 11. Resolute FJ

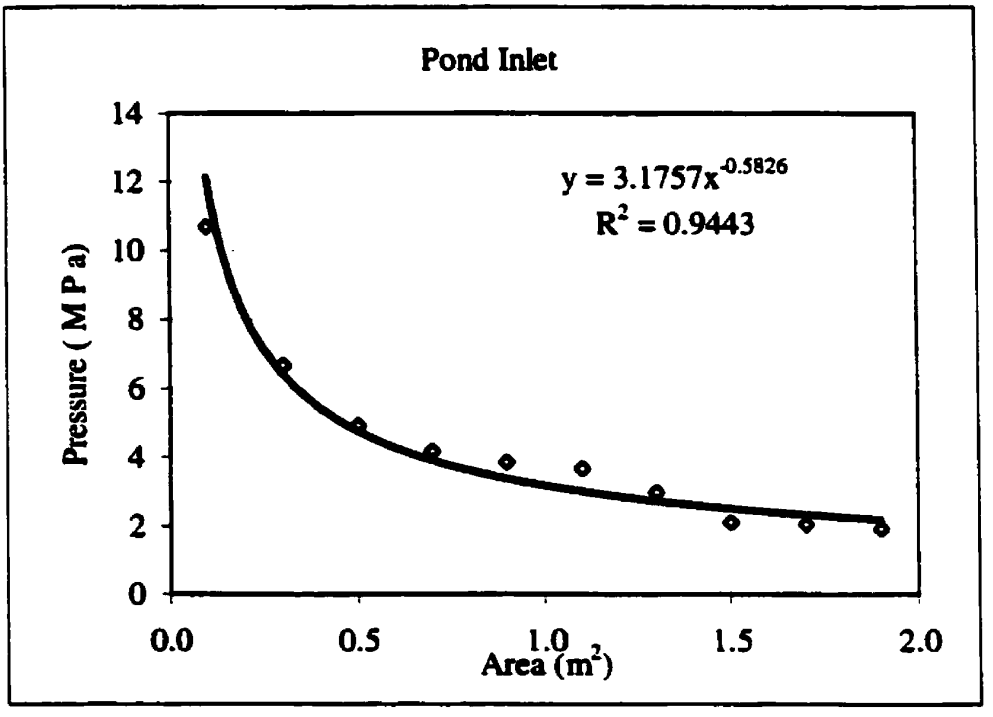

Figure 12. Pond Inlet

The values of the coefficients were given in the table below

DATASET	DESCRIPTION	$P = C_1 A^{-C_2}$	
		C_1	C_2
1	Hobson's Choice '89	6.2251	0.4359
2	Hobson's Choice '90	5.1163	0.1863
3	Polar Sea	5.394	0.4183
4	Kigoriak Aug '81	1.5778	0.4273
5	Kigoriak Oct '81	1.6671	0.6616
6	M. V. Arctic '84	4.1751	0.3618
7	Resolute FJ (flat jack)	5.032	0.4118
8	Pond inlet	3.1757	0.5826

Figure 13. Coefficients C_1 and C_2

The coefficients C_1 and C_2 were analyzed to see if they were statistically distributed. Each set of data was given the same weight. Different distributions were tested and a Weibull plot was fitted to the data. The cumulative distribution function for 2-parameter Weibull distribution is

$$y = F(x) = 1 - \exp\left[-\left(\frac{x}{\delta}\right)^{\beta}\right]; x > 0 \qquad (2)$$

In the above expression x is the coefficient, β is shape parameter and δ is scale parameter (e.g. Castillo, 1988). The mean and standard deviation were then determined from the parameters of the Weibull distribution. The expressions for mean and variance of a 2-parameter Weibull distribution was given by

$$Mean = \delta\Gamma\left(1 + \frac{1}{\beta}\right) \qquad (3)$$

$$Variance = \delta^2\left[\Gamma\left(1+\frac{2}{\beta}\right)-\Gamma^2\left(1+\frac{1}{\beta}\right)\right] \tag{4}$$

The standard deviation was then calculated from the variance. Based upon the above expressions the mean for C_1 was 5.16 and standard deviation was 3.716; for C_2 mean was 0.4090 and the standard deviation was 0.1313. The Weibull plots for coefficients C_1 and C_2 are given in Figures 14 and 15.

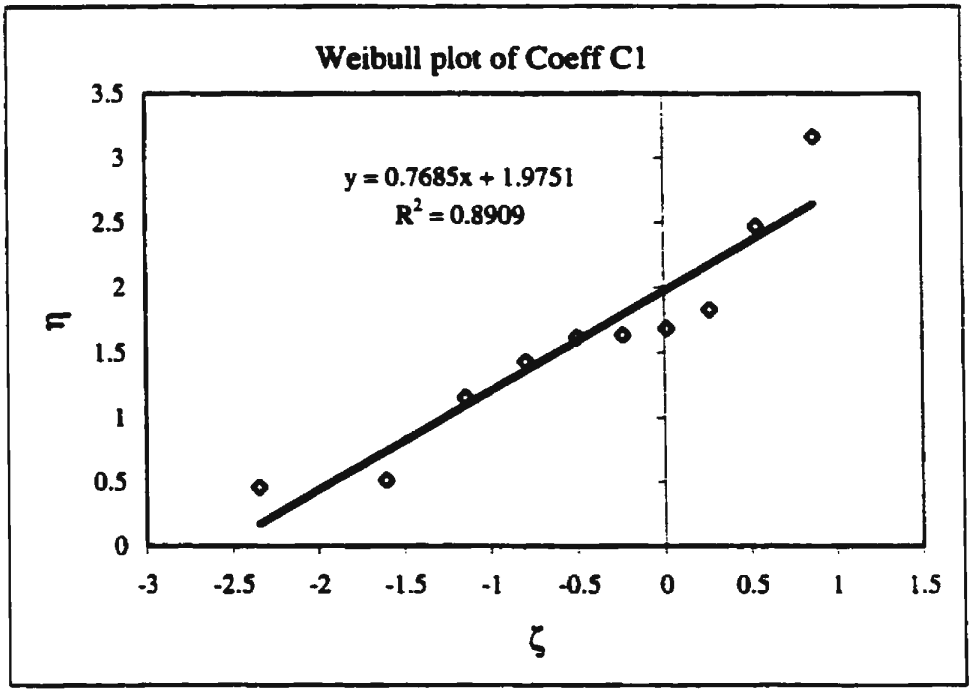

Figure 14. Weibull Plot of Coefficient C_1

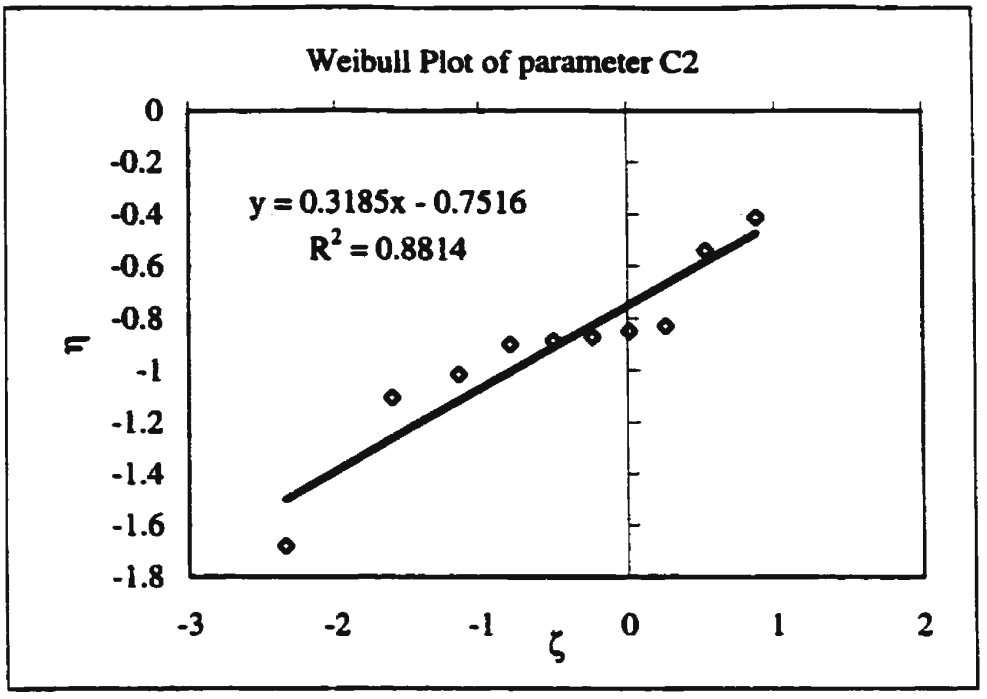

Figure 15. Weibull Plot of Coefficient C_2

Based upon the values of mean and standard deviation, the expression to predict the value of the contact pressure at a given contact area can be formulated as.

$$P = 5.16A^{-0.4090} \tag{5}$$

Now by taking 95% confidence interval the values of C_1 and C_2 were calculated. The equation after taking into consideration 95% confidence interval is

$$P = \begin{pmatrix} 2.585 \\ 7.735 \end{pmatrix} A^{-\left(\frac{0.3181}{0.5001}\right)} \tag{6}$$

The above expression for pressure predicts with 95% confidence that the value of C_1 lies between 2.585 and 7.735 and the value of C_2 lies between –0.3181 and –0.5001.

Using equation (6) the pressure values were calculated for the data used in the above analysis and the plot is shown in Figure 16. The equation predicts pressures more accurately when the contact area was less than 2 m^2, since the statistical analysis uses only those contact pressures when the contact area is less then 2 m^2.

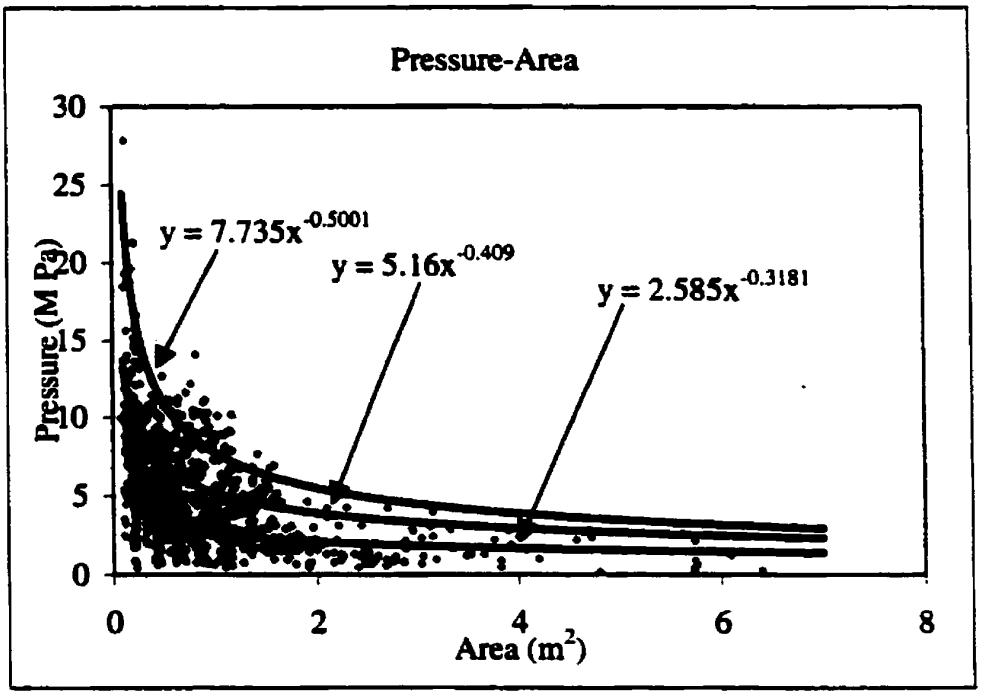

Figure 16. Pressure-Area taking all the data used in the statistical analysis

The expression given in equation (6) estimates the maximum pressure values for contact areas less than $2m^2$. It was used to predict the values of ice pressure for the contact areas less than $2m^2$ in the data sets given above and it gave a good fit with an R^2 value of 0.946. The graph is given in Figure 17.

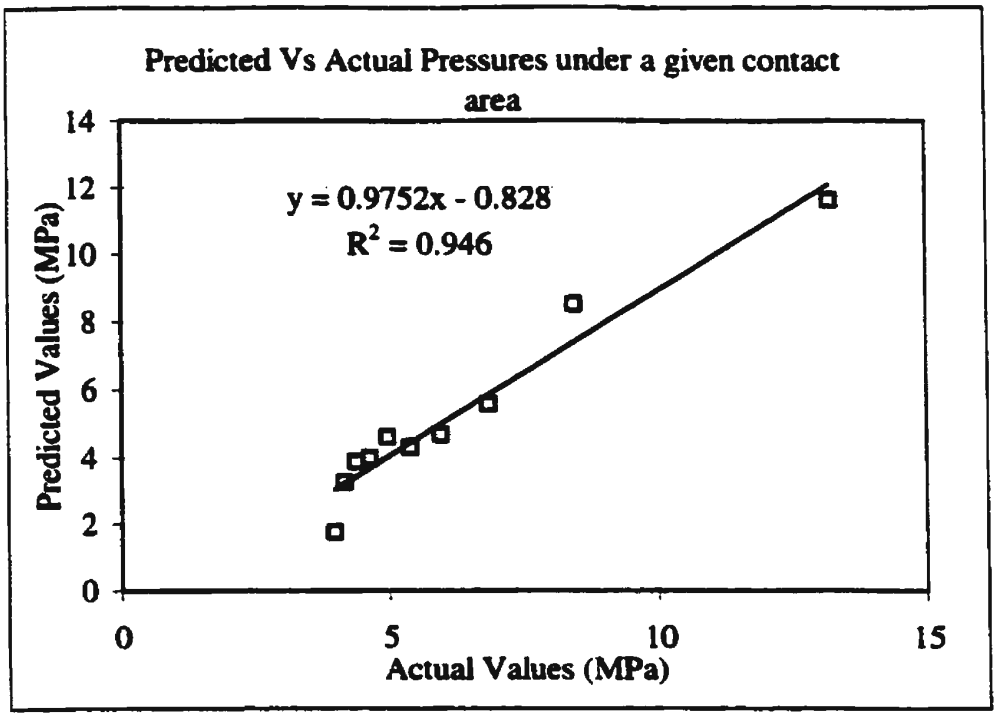

Figure 17. Predicted Against Actual contact pressures (At areas between 0.1 m^2 and 2 m^2)

The standard error in the above predictions can be calculated as

$$S_{y.x} = \frac{\sum_{i=1}^{n}\left(Y_i - \hat{Y}_i\right)^2}{n-2} = 0.698 \qquad (7)$$

In the above formula $S_{y.x}$ measures the variation in the predicted values with respect to the actual values of the pressures. From the standard error the percentage error in the predictions can be estimated by taking the ratio of the standard error and the average value of the pressures. The standard error is $\frac{0.698}{6.198} = 0.113$. That is 11.3%.

2.3 Regression Analysis

There has been an argument amongst researchers about the factors (aspect ratio, indentation rate and temperature of ice), affecting ice pressures other than contact area. To study this issue a regression analysis was carried out using the available data from various laboratory scale experiments. The analysis indicated that the effect of various factors other than contact area was minimal and can be ignored. However the details of the analysis are given below for interest.

Landanyi (1967) formulated an expression for maximum pressure on an indentor by ice. This is given as

$$P = \sigma_c \left(3\frac{(1+\nu)\sigma_c}{2E} F + \varepsilon_{av} \right)^{-a} \tag{8}$$

where,

$$a = \frac{2}{3}\left(1 - \frac{1}{f}\right) \text{ and} \tag{9}$$

$$F = \frac{2}{9(m+1)}\left(m - 1 + 6\left[1 - \frac{2}{9}(m-1)^2\right]^{1/2} \right) \tag{10}$$

Here

f is1.6, $m = \frac{1}{\nu}$, ν = Poisson's ratio =0.33 ± 0.03, σ_c = Uni-axial compressive strength of ice and ε_{av} can be taken as zero. The above equation on simplification gives

$$P_{max} = 10.34\sigma_c^{0.75} \tag{11}$$

The above expression does not take into account various factors outlined above such as aspect ratio, compressive strength of ice, etc., To study these effects a general form of the above expression was assumed eliminating the constant value 10 and replacing it with k, and is written as

$$P_{indent} = k\sigma_c^{0.75} \tag{12}$$

The value of k in the above expression depends on various factors effecting the ice loads on structures such as area of contact, aspect ratio and indentation rate. The value of k is determined from the data reported by Timco (1986), Sodhi (1991, 1992) by performing a regression analysis. The value of k from regression is

$$k = 30 \times \left(\frac{D}{h}\right)^{0.35} (A)^{0.7} \left(\frac{U}{D}\right)^{0.09} \tag{13}$$

The above equation can be used only for aspect ratios less than 2.The model was used to check the existing results but does not produce satisfactory results. So it was assumed that the major player in determining the contact pressure is the contact area and the effects of any other parameters are minimal.

Chapter 3

Development of Simulation Model

3.1 Introduction

The model developed in the preceding section (equation 5) was incorporated into a Fortran program, STEADY developed by Veitch (1995). The main goal of the simulation model was to predict the propeller-ice contact forces on propeller blades and shaft. The ice was held fixed in the simulation process to model the indentation process and to eliminate any momentum effects due to the motion of the ice.

3.2 Development of a simulation model for interaction between stopped propeller and ice

The propeller used in the simulations is that of the *R-class* icebreaker. Discretization of the propeller geometry was done in a separate Fortran program called DISCRT. It gives the coordinates of the points on the propeller surface, and the local blade section angles, unit normals and incremental areas of each point. The number of points in the discretization can be defined by using cubic spline fitting and interpolation routines (Press et al. 1987).

Each simulated event is defined by the initial conditions of the ice and propeller. It is possible to assign any position and velocity values to either body. The ice was held stationary. The propeller has constant forward velocity and the rotational velocity is zero.

The major changes were made in INTERFM subroutine of the simulation program. Its main function is to calculate check the points of intersection between the propeller and ice and calculate the pressure distribution. In the modified version, the way it calculates the pressure was changed. In the earlier version of the code, contact pressures were determined first by using the contact model developed by Veitch (1995) to calculate the forces and moments. In the modified version, the contact areas were determined based on the contact geometry and were used to calculate the contact pressures. The forces and moments were determined from the pressure values.

The simulation program starts with a **MAIN** module which calls on the **CONTROL** module which does the main simulation process. The **CONTROL** module calls on the input subroutines to load different parameters such as physical conditions, Initial conditions of ice (location and orientation), initial conditions of the propeller (location, and velocity) and the propeller geometry. It then calls on **ICECONT**, which performs the time stepping indentation procedure. An initial time value is assigned here and the simulation routine is started by calling different subroutines **PROPMOVE**, **LOCATE**, **FIRSTHIT**, **PASSONE** and **INTERFM** to check the position of the propeller, locating its position with respect to ice, calculate the section angles and to determine the points of contact, calculate the areas of contact, determine the contact pressure and calculate the

forces and moments on propeller shaft and blades. The control is passed on back to **CONTROL**, which calls on **FMOUT** to write the results. The general description of all the subroutines is presented below. The flow chart of the simulation program is presented in Figure 18.

3.3 Program structure

MAIN is the main program module. It sets common areas and counters. Calls to **CONTROL** for program execution.

CONTROL controls the execution sequence of the steady state ice cutting procedure (where the ice was held stationary) Calls on input subroutines to read in data & on **ICECONT** drives the time stepping ice cutting procedure and calls on **PROPMOVE**, **LOCATE**, **FIRSTHIT**, **PASS** and **INTERFM**. It Stores the return results in the common area **/FMSAVE/**.

PROPMOVE calculates the current position & orientation of the propeller axes in space

LOCATE calculates the position of the ice axes' origin in the propeller axes system.

FIRSTHIT determines which blade makes first contact & then calls on PASS.

PASS calculates the angle of attack for each blade section.

INTERFM determines the points of intersection between the ice & propeller, calculates the local contact areas by adding all the incremental contact areas, and then evaluates the local pressure as a function of the contact area. Forces, and moments at each point are calculated and summed & transformed to the ice axes. Thus, F & M in both propeller and ice axes are determined

INPHYS reads in physical constants & ice diameter from file **CONSTANT.DAT**

INICE reads in initial conditions of ice from file **INITICE.DAT**

INPROP reads in propeller geometry from file **PROPGEOM.DAT** and the initial conditions of propeller from file **INITPROP.DAT**

FMOUT writes propeller position & orientation, propeller contact force & moment components, ice contact force & moment component and time: all as functions of time, to file **CUTOUT21.DAT,** writes a summary of the propeller loading to a file **STEADYP.DAT**

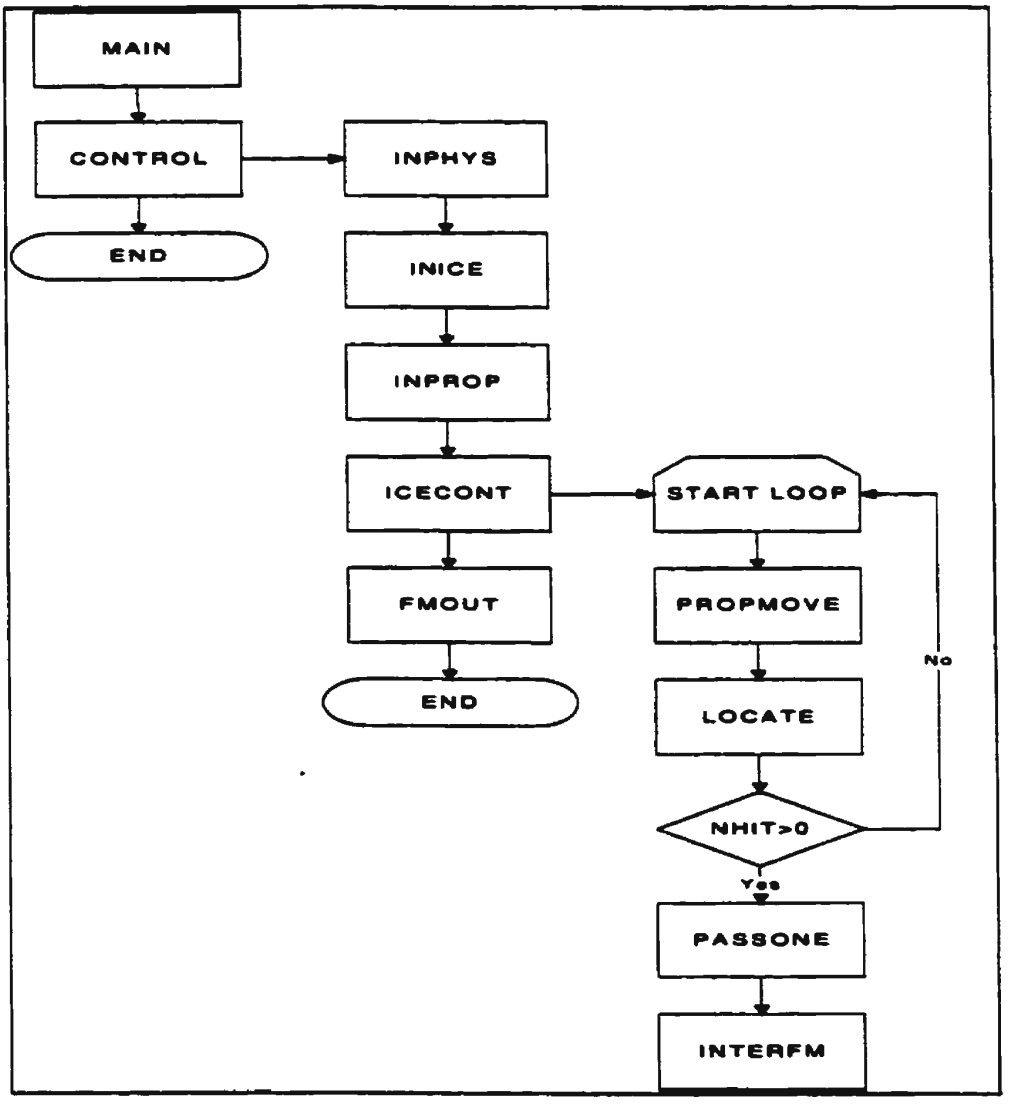

Figure 18. Program Flow chart

3.4 Simulation Predictions

In this section, predictions made with the model developed in the preceding section were discussed. The main goal of this model was to predict the ice loads on a propeller blade when the propeller was stopped and was pushed into the ice.

Case 1

Propeller-ice indentation process was simulated for the case of zero rpm. The velocity of indentation was 1 m/s. As the contact pressure is dependent on contact area according to the contact model, five different depths of indentation were chosen and the ice diameter was chosen as three times the blade span. The initial positions of the propeller and ice were given, along with the constant values of ρ_i, ρ_w in the input files.

For every simulation, time histories of several items were stored in data files. The propeller shaft thrust and torque loads and the blade loads such as blade bending moments (in plane and out of plane) and spindle torque were saved. The forces acting on the ice due to propeller indentation were also saved. An example of time histories made by the simulation program is shown in the Figures 19 through 21. The time histories presented were for a case when the depth of indentation was 65 cm.

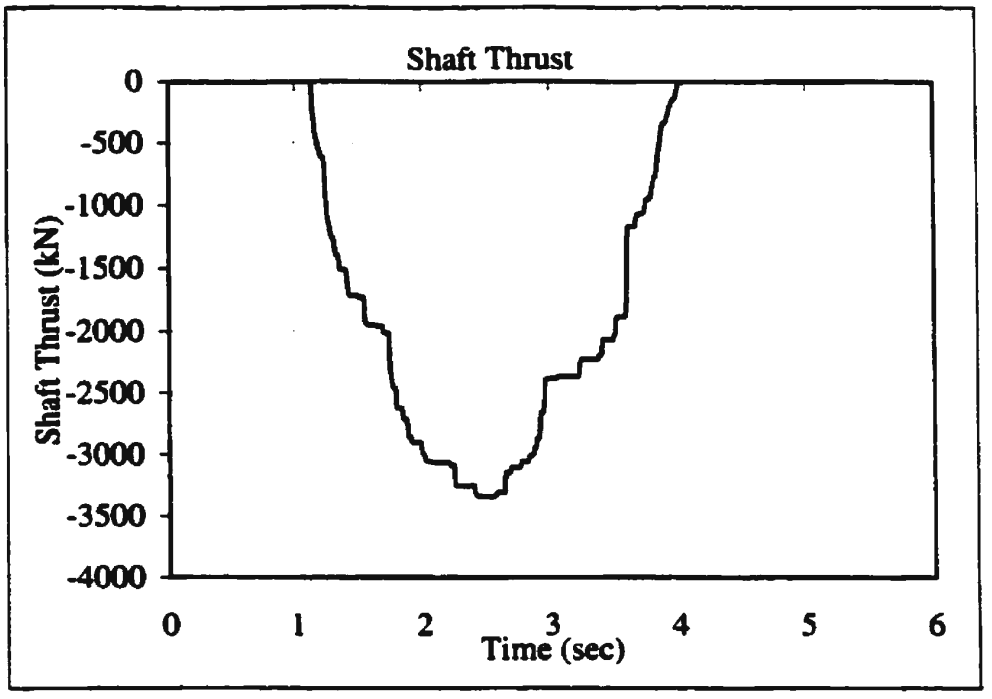

Figure 19. Shaft Thrust

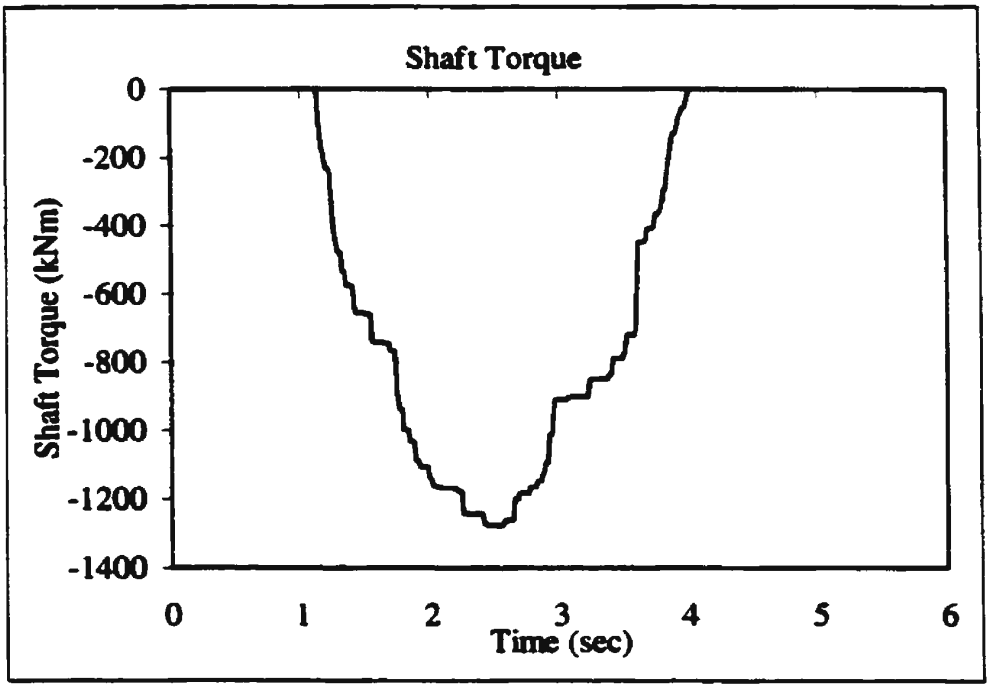

Figure 20. Shaft Torque

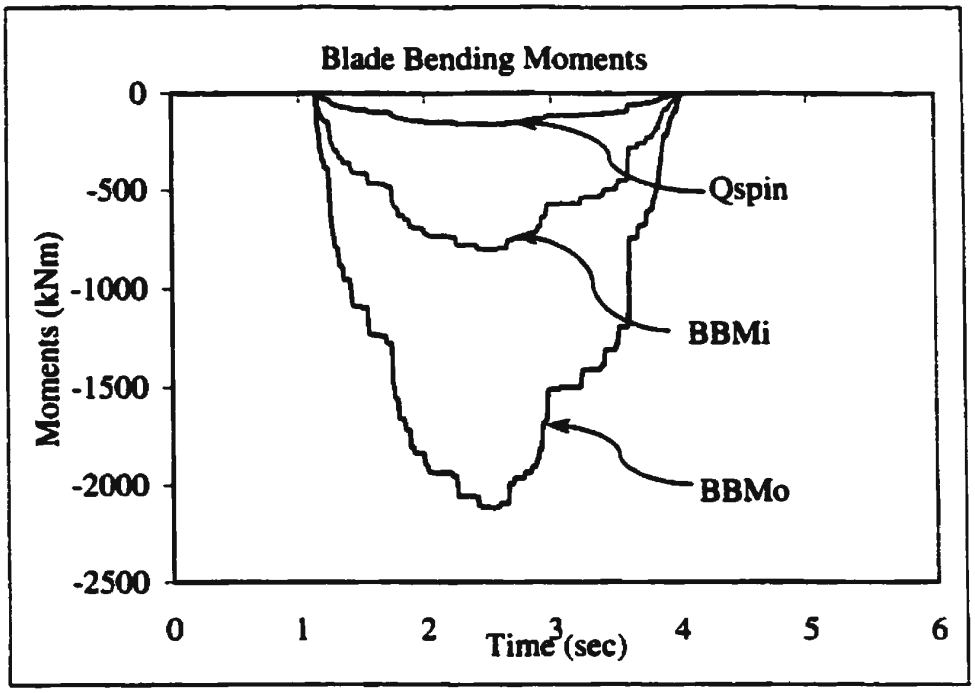

Figure 21. Blade Bending Moments

In Figure 19, the shaft thrust was plotted against time. One blade contact was made with the ice, as the propeller was not rotating. The contact results in a negative shaft thrust. The hydrodynamic load was zero because the propeller was not rotating. In Figure 20, shaft torque was plotted against time and was negative. In Figure 21, the blade bending moments are plotted. The in-plane blade bending moment (BBMi), out of plane blade bending moment (BBMo), and the spindle torque (Qspin) are plotted against time. In this case the smallest moment is Qspin, the largest is BBMo and BBMi is in between. The simulation case deals with ice indentation when the propeller blade acts as a cantilever with a large load applied on it. This results in a large bending moment. This also agrees with most full-scale measurements as maximum loads are out of plane blade bending moments. Time histories were obtained for all the simulation cases. But rather

than time histories, the trends followed by the forces and moments with the change in depth of indentation were represented as the depth of indentation plays an important role in determining ice forces on propeller blades.

The maximum contact thrust loads were plotted against depth of indentation. The propeller forces and the moments were considerably sensitive to the depth of indentation and increased with the increase of the depth of indentation. The sensitivity varied almost linearly with the depth of indentation. As the depth of indentation increases, more blade area comes into contact with ice, which in turn results in higher shaft thrust and torque values. It was observed that the loads increased by 4 times when the depth of indentation was increased by 4 times. Similar increases in the shaft torque and blade-bending moments were observed. The results are presented in Figures 22 through 26.

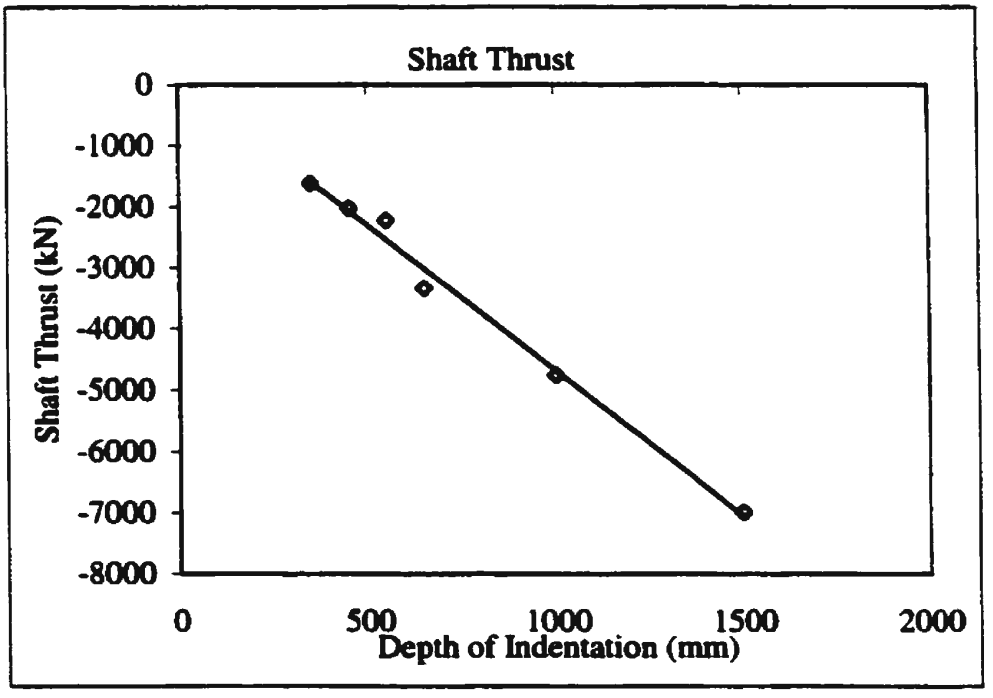

Figure 22. Shaft Thrust

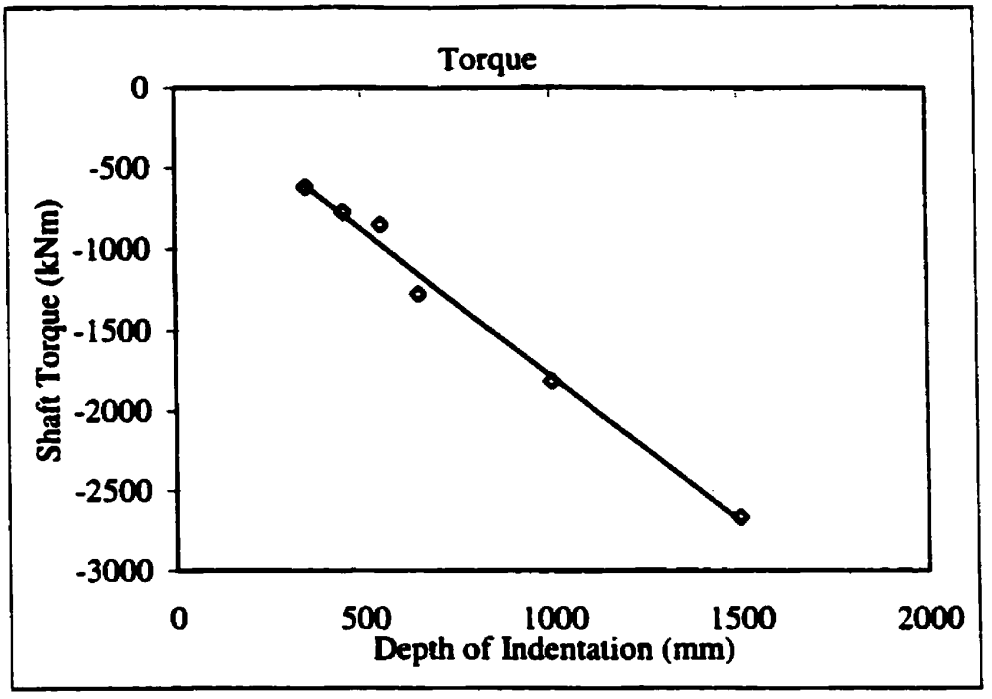

Figure 23. Shaft Torque

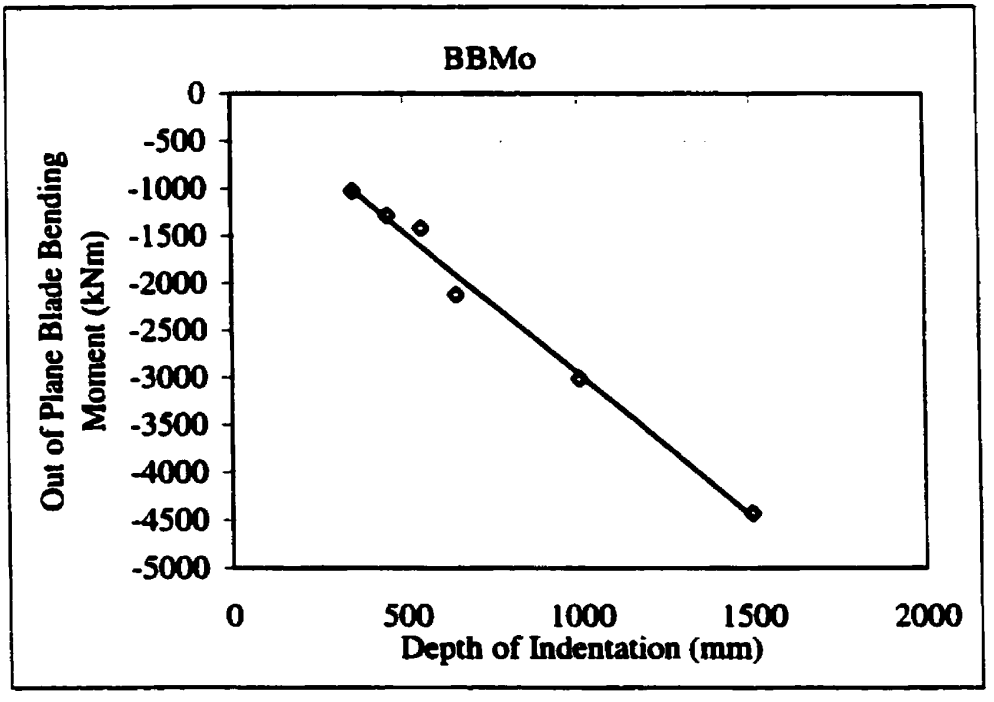

Figure 24. Out of Plane Blade Bending Moment

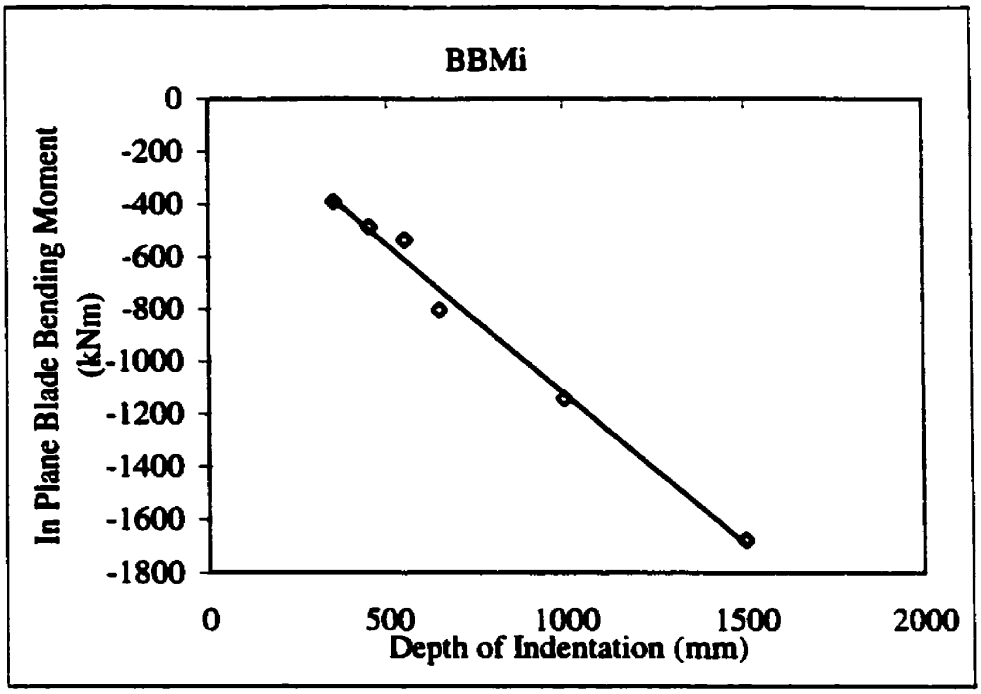

Figure 25. BBMi

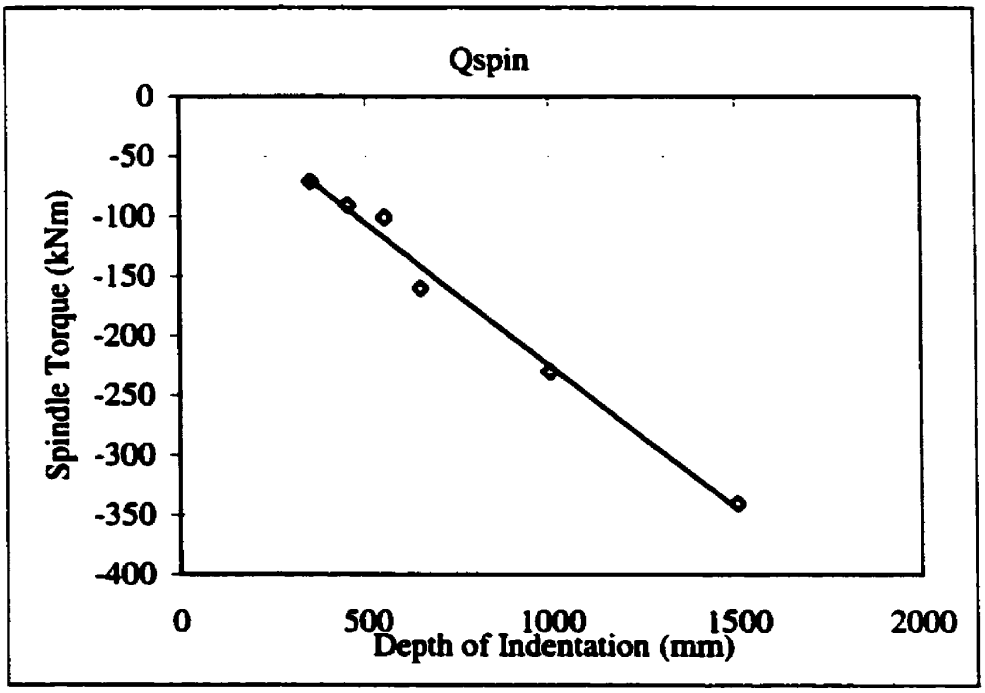

Figure 26. Spindle Torque

Case 2

The movement of the ice in seawater has a considerable effect on propeller loads. When a propeller indents into a semi-infinite (very large in size in comparison to the diameter of the propeller) piece of ice, a continuous indentation process takes place. But if the ice was relatively small and was free to move, the effect of it on the propeller blades is minimal. In practice during the ship ramming cycles the propellers were stopped for a short period to change the ship's course. At this point, the stopped propellers may come into contact with submerged ice pieces broken by the ship. In some cases the propellers may come into contact with semi-infinite ice pieces, which cause severe damage to propeller blades.

To study the effect of the motion of ice, this process was simulated with a modified version of the code for full motion simulation developed by Veitch (1995) in which the ice was free to move. In this program the modifications were made in the INTERFM subroutine, the details of the modifications were already described in the previous case. The vertical motion of the ice was arrested by equating the densities of seawater and ice, to maintain a constant depth of indentation.

The simulations were done with the same input conditions used in the previous case, such as depth of indentation, velocity of indentation and ice size. The depths of indentation chosen were 350, 450, 550, 650, 1000 and 1500 mm. The velocity of indentation was 1 m/s. The size of the ice was 3 times the blade span. It was observed that there was considerable variation in the forces and moments on propeller

shaft and the blades. The value of the shaft thrust was 10 times smaller when the ice was free to move at 350 mm depth of indentation and it was 3 times smaller at 1500mm depth of indentation. The shaft torque varied considerably. It was 20 times smaller at 350 mm depth of indentation and 9 times smaller at 1500 depth of indentation. The out of plane blade bending moment was 10 times smaller at 350 mm depth and 6 times smaller at 1500 mm depth. The value of in-plane blade bending moment was 10 times smaller at 350 mm and 4 times smaller at 1500. The motion of the ice has no considerable affect on spindle torque. The plots are presented in Figures 27 through 31.

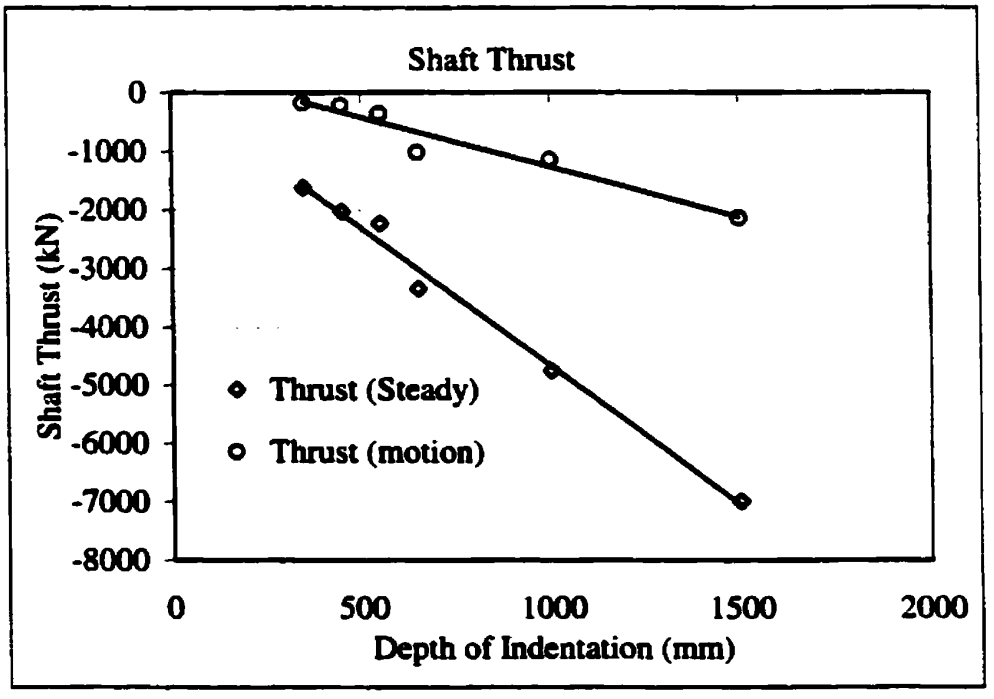

Figure 27. Shaft Thrust

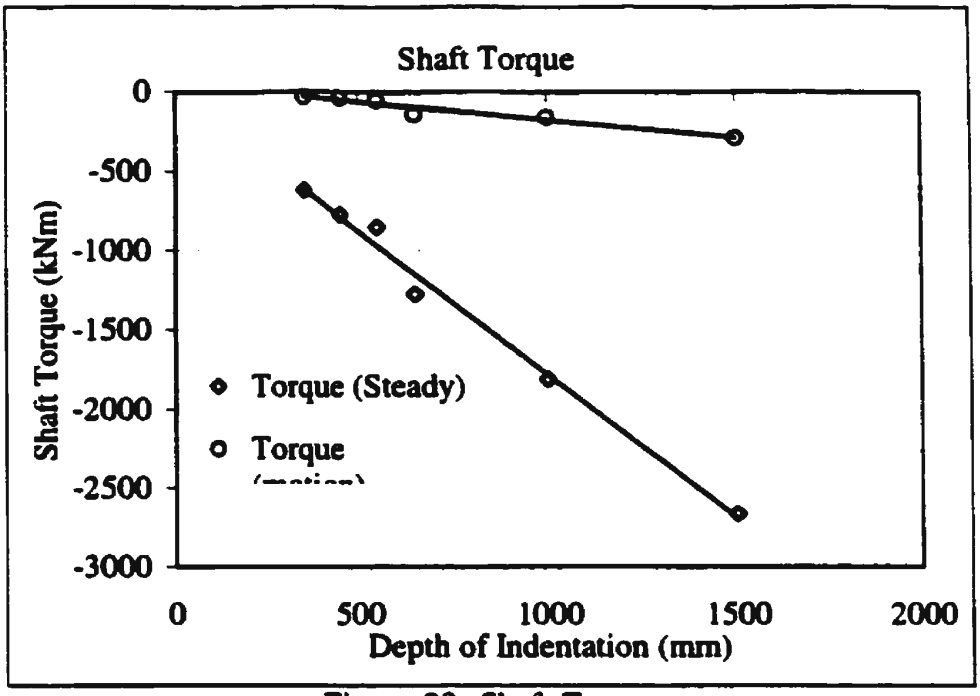

Figure 28. Shaft Torque

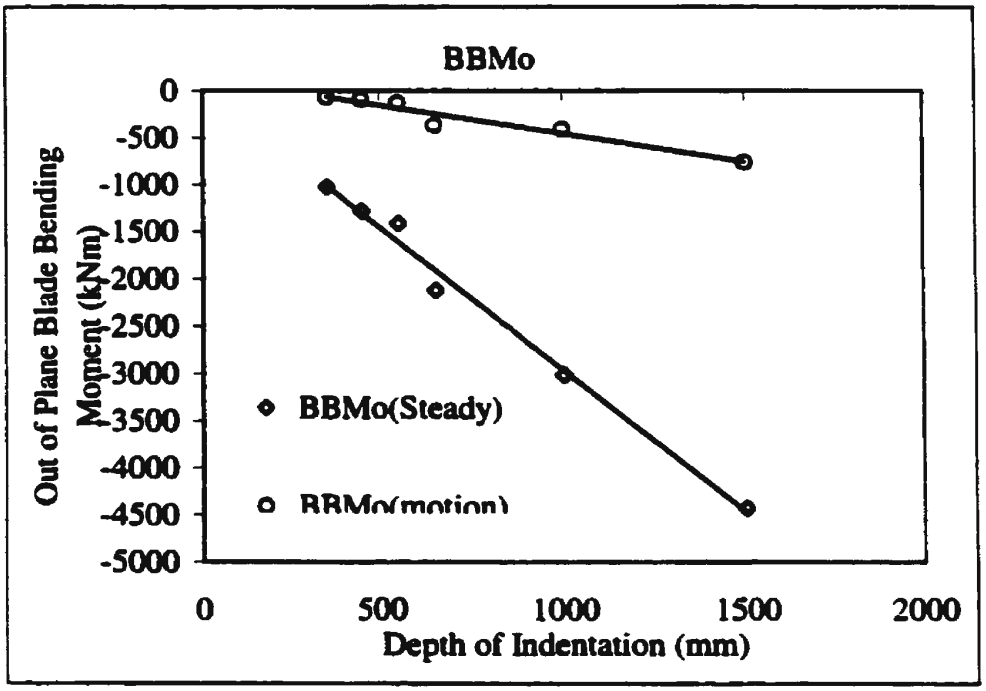

Figure 29. Out of Plane Blade Bending Moment

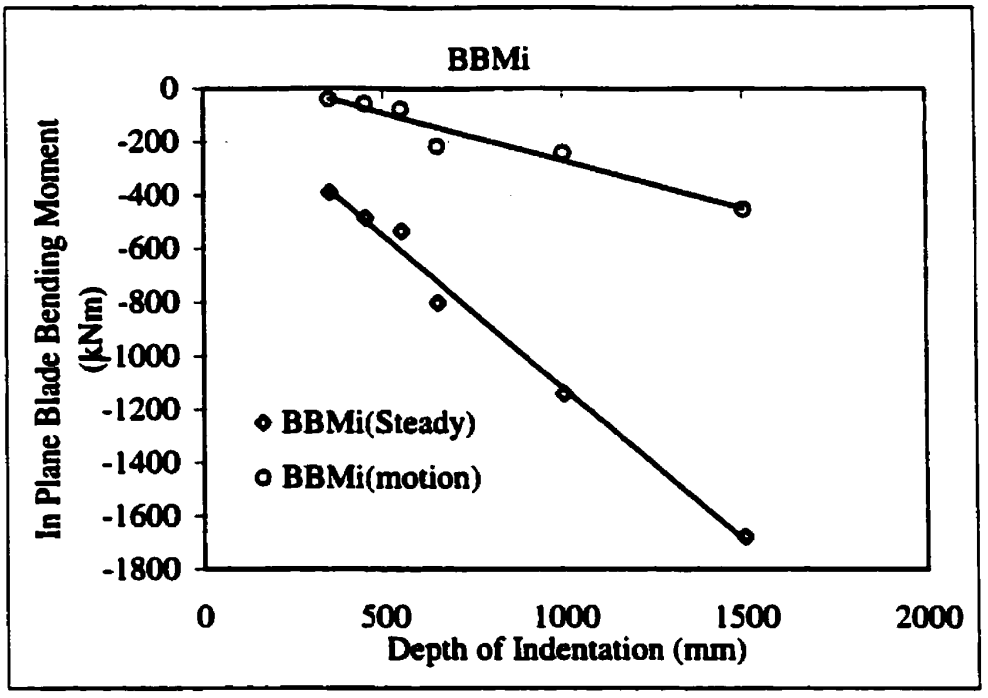

Figure 30: In Plane Blade Bending Moment

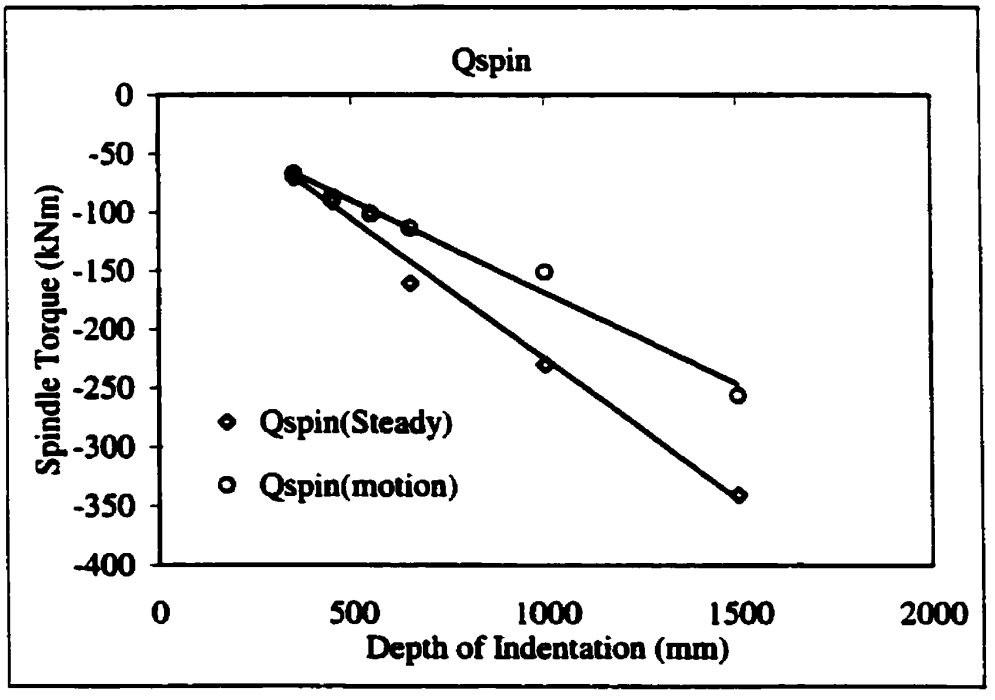

Figure 31: Spindle Torque

Case 3

The geometry of the propeller has a considerable effect on ice loads. The size of the propeller, its skew and pitch distributions affect the ice loads. To check the effect of propeller geometry, simulations were performed using steady state version of the program, using a series of propellers. The propellers used were *R-Class, Caribou, Louis St. Laurent* and *B* (name of this propeller is confidential). As the propellers varied in sizes and geometries, the forces and moments were non-dimensionalised. New coefficients were formulated for all the forces and moments and are given below

$$I_T = \frac{T}{\rho g D^3} \tag{14}$$

$$I_Q = \frac{Q}{\rho g D^4} \tag{15}$$

$$I_{BO} = \frac{BBMo}{\rho g D^4} \tag{16}$$

$$I_{Bi} = \frac{BBMi}{\rho g D^4} \tag{17}$$

$$I_S = \frac{Qspin}{\rho g D^4} \tag{18}$$

where, I_T is coefficient of shaft thrust due to indentation, I_Q is the coefficient of shaft torque due to indentation, I_{BO}, I_{Bi}, I_S are coefficients of out of plane blade bending moment, in plane blade bending moment and spindle torque respectively, T is shaft thrust, Q is shaft torque, *BBMo, BBMi, Qspin* are out of plane blade bending moment, in plane blade bending moment and spindle torque respectively, ρ is density, g is the

acceleration due to gravity and *D* is the diameter of the propeller. These coefficients were plotted against *d/D*, where *d* is the depth of indentation. In general, it was observed that with increase of d/D the values of thrust, torque and blade bending moment coefficients increased.

The plots of the coefficients mentioned above are presented in Figures 32 Through 36. The propeller-ice coordinate system is given in Figure 37.

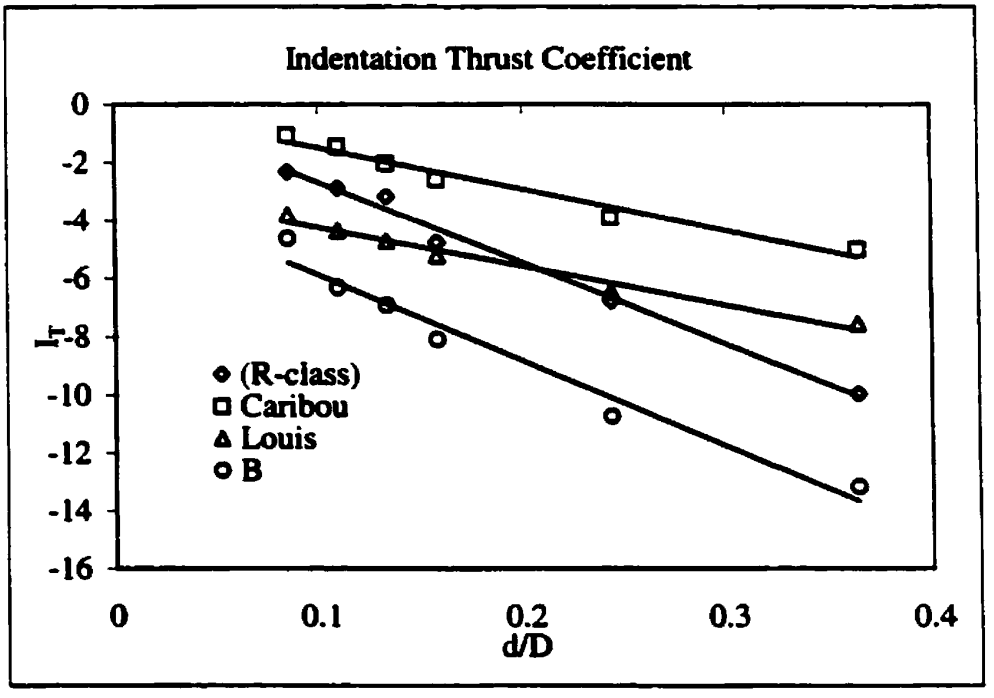

Figure 32. Indentation Thrust Coefficient

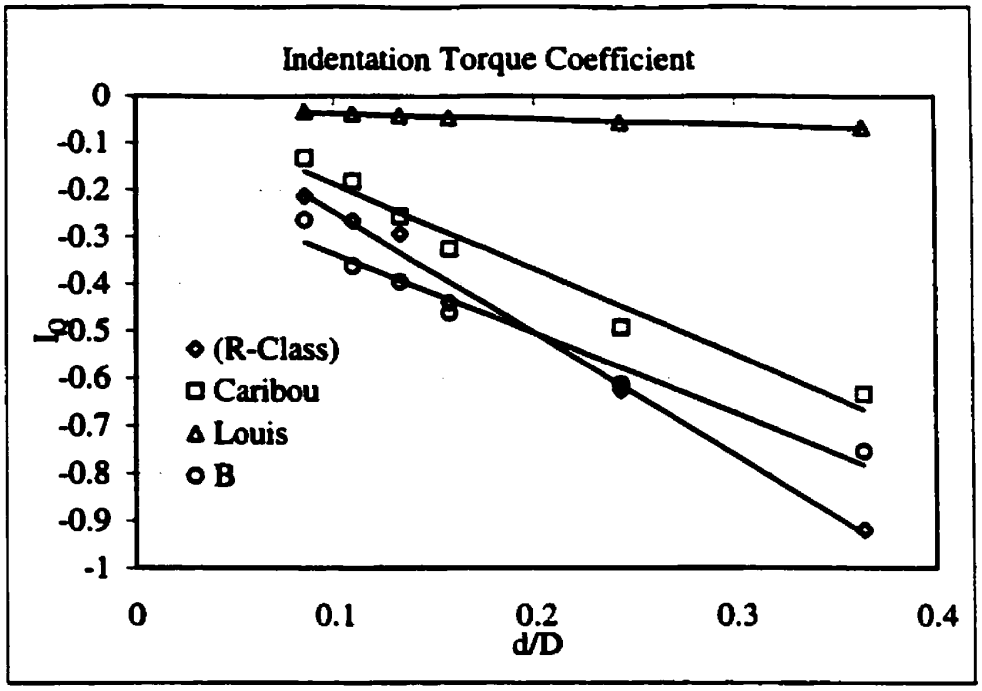

Figure 33. Indentation Torque Coefficient

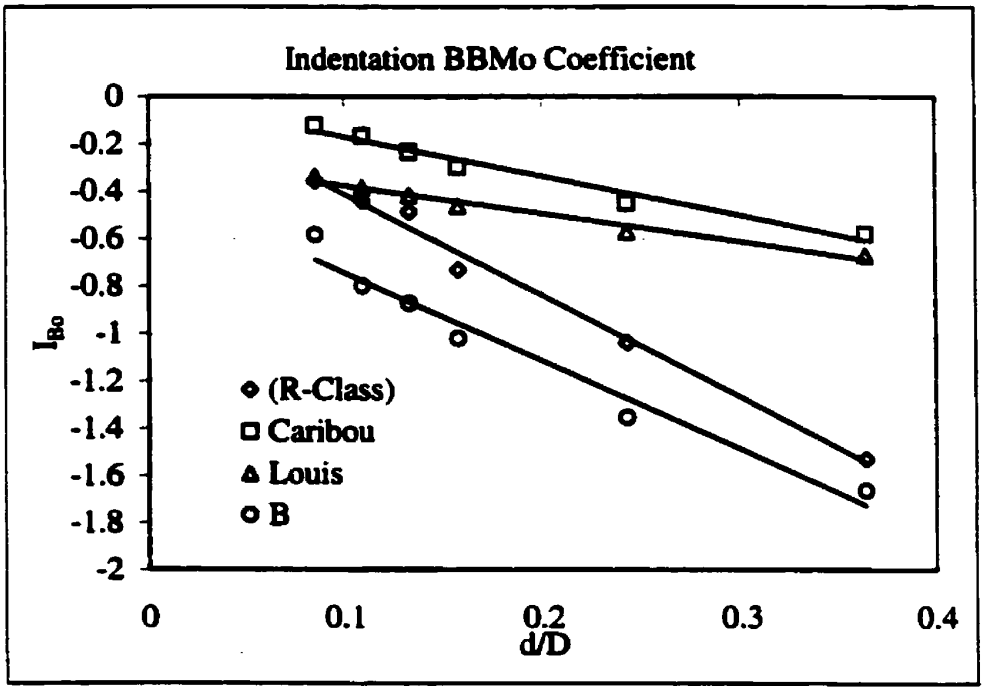

Figure 34. Indentation BBMo Coefficient

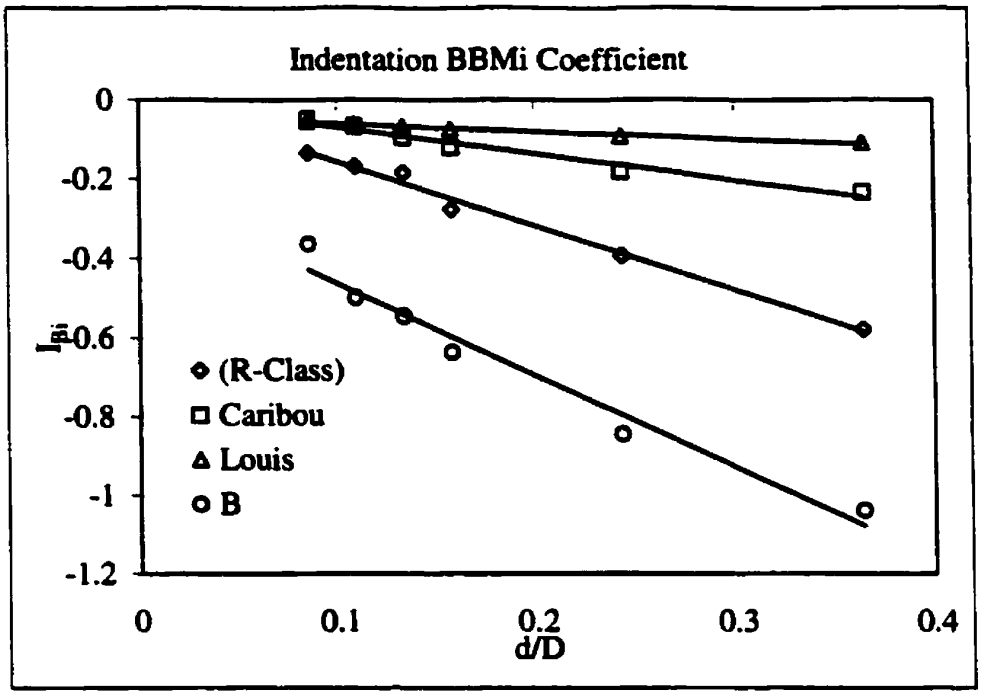

Figure 35. Indentation BBMi Coefficient

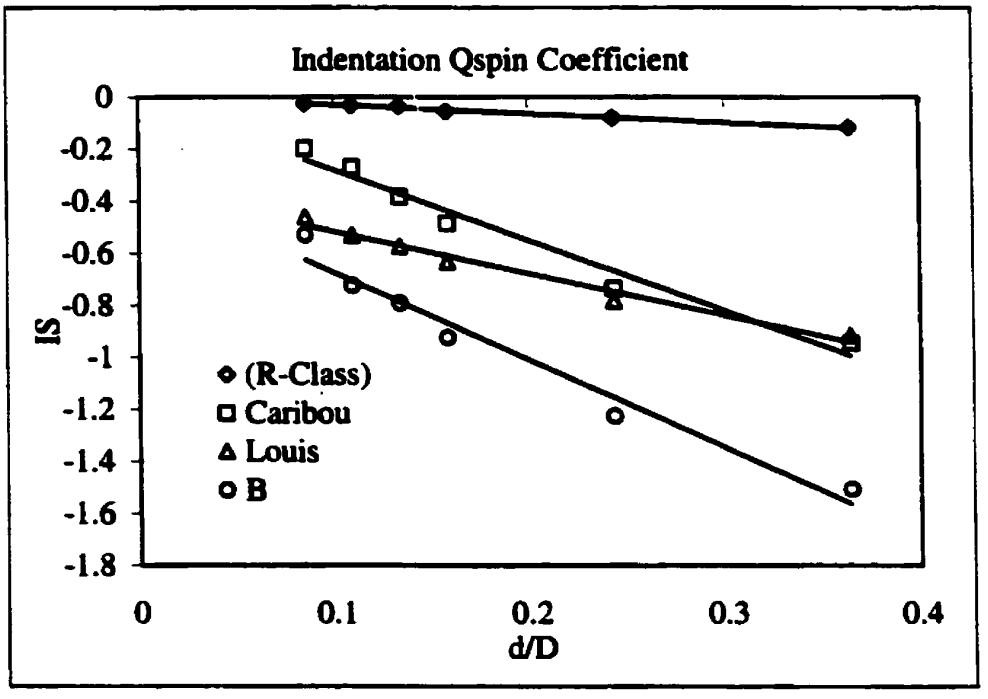

Figure 36. Indentation Qspin Coefficient

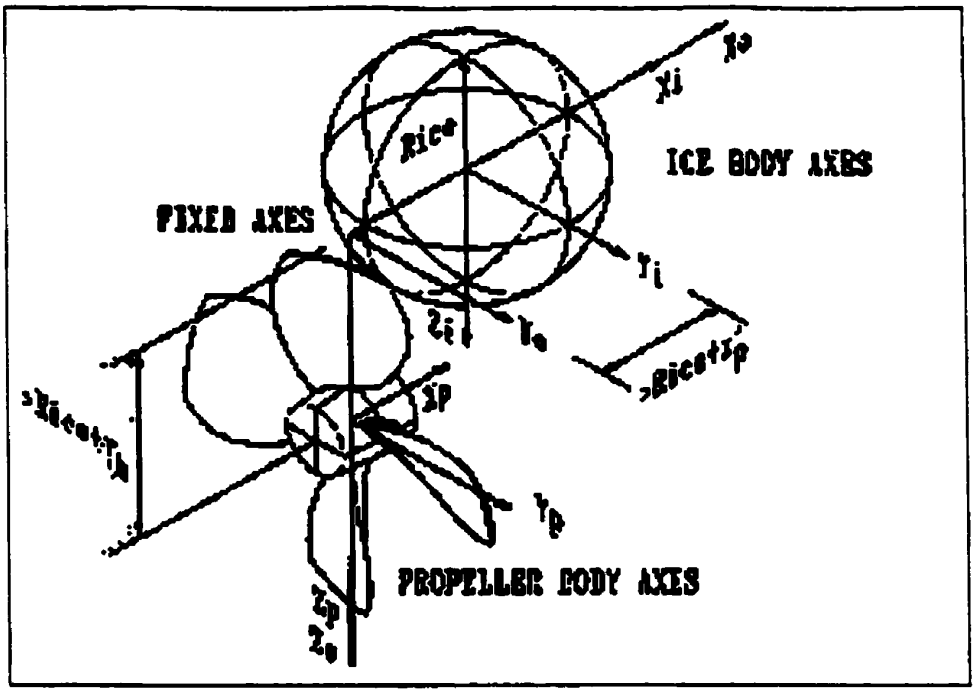

Figure 37. Propeller-ice coordinate system (courtesy Veitch (1995))

Chapter 4

Experimental Program

4.1 Aim

The model developed in chapter 2 was used to predict ice loads on propellers during propeller-ice indentation process. To verify the correctness of the model a series of small-scale indentation tests were performed at the Institute of Marine Dynamics (NRC). The tests were performed using an indentor whose surface was a scaled version of the suction side of the *R-Class* propeller blade. EG/AD/S model ice developed by NRC was used for testing. The tests were performed using a high speed MTS (Material Testing System).

4.2 Background

The main purpose of these experiments was to investigate the ice loads on propellers during propeller-ice indentation process, which is the interaction between a stopped propeller and ice. To study the effect of ice when the propellers were rotating at small rotational speeds the angle of the indentor was varied with the use of wedges connected to the indentor. The description and use of wedges is given later in this chapter.

4.3 Experimental Program

The experimental program consisted of a total of 72 experiments. The test matrix is given in the table below.

Wedge Angle(Degrees)						
Depth of Indentation	0°			10°	20°	30°
(mm)			Velocity of Indentation (m/s)			
	0.5 m/s	0.7 m/s	1m/s	1m/s	1m/s	1m/s
35mm	4	4	4	4	4	4
45mm	4	4	4	4	4	4
55mm	4	4	4	4	4	4

The main varying factors of the test program were depth of indentation, which is the length along the blade span from the tip that was in contact with the ice as illustrated in Figure 38, velocity of indentation and the angle of the wedge. The temperature was maintained at -6^0 C throughout the testing. The tests were of three different series.

Series1: Constant depth of indentation over a range of indentation angles (to determine the effect of indentation angle)

Series 2: Constant depth of indentation over a range of velocities of indentation

Series 3: Constant indentor angle over a range of depths of indentation

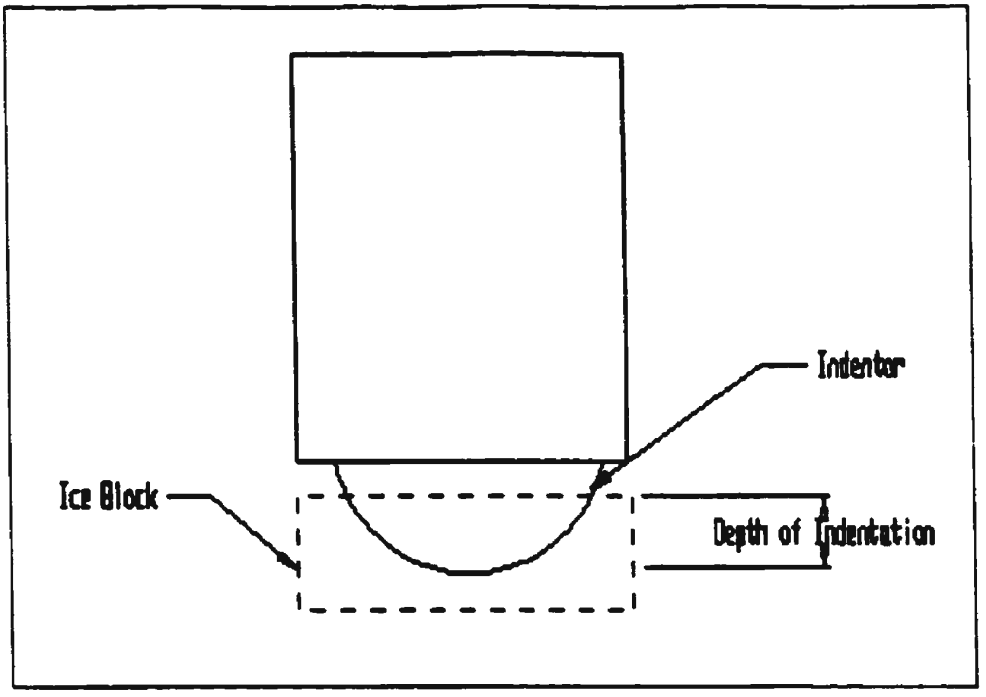

Figure 38. Depth of Indentation

4.3.1 Facilities

The experiments were done in the large cold room at the Institute for Marine Dynamics (IMD) of the National Research Council of Canada (NRC). The cold room is divided into two parts. The testing apparatus was located in the first part and the sample preparation was done in the second part. Both rooms are equipped with an evaporator, which enables a constant temperature between 0° C and –40° C to be maintained. The temperature was maintained at –6°C in both the rooms throughout the testing process.

An adjacent warm up room contains the control console of the testing apparatus, signal conditioning, data acquisition device and computer. There is a glass window fitted to the wall of the warm up room, which can be used to observe the testing process.

4.3.2 Ice source and Storage

The ice samples were collected from a 110 mm thick sheet of EG/AD/S (Ethylene Glycol (0.39 %)/Aliphatic Detergent (0.036 %)/ Sugar (0.04 %)) model ice from the ice tank of IMD. The EGADS mixture produces a much softer ice than fresh water ice. Bubbles are added to the ice to control its density.

For the preparation of the ice, the ice tank was cooled to about –19° C and warm water was sprayed into the air to form an ice crystal fog, which slowly falls to the cold water surface. Each tiny crystal then acts as a seed to form an ice column. This process is called seeding.

The collected ice samples were 360 mm × 260 mm × 110 mm. After the ice samples were cut into the required dimensions, they were laid on a wooden mesh to drain out the excess water and were then stored in plastic garbage bags and were tagged and numbered. The samples were then shifted to the storage area (small cold room at IMD), which was maintained at – 15° C.

4.3.3 Test Apparatus

The testing was done on a high speed MTS machine at IMD. This machine provides a uni-axial, compressive force by means of a hydraulic actuator. It has three main parts: a

frame, a hydraulic circuit providing the force and a control console for the control of the actuator and signal conditioner.

The frame is made with a base, which contains an actuator, and a crosshead held by four posts and able to move along a vertical axis. The crosshead is lifted and locked on the posts manually. The actuator has a capacity of 250 kN in both tension and compression. The indentor setup was attached to the crosshead. A box closed on three sides was attached to the bottom frame, in which the ice block was placed. The box was used to confine the ice from movement during the indentation process.

The hydraulic power supply is located in the mechanical room above the cold room. Hydraulic oil runs down to the actuator and back up to the oil tank. A high-pressure pump supplies pressure. The parts of the hydraulic line in contact with cold air are insulated and were continuously heated in order to avoid high temperature gradient or freezing of the oil.

An inline piezoelectric load cell (which was a highly accurate load cell connected to the testing apparatus to verify the loads measured by the six component load cell) was connected to a dual mode integrating amplifier, which was connected to a strain gauge conditioner and amplifier. The six component load cell AMTI MC6-6-4000 and the LVDT were also connected to the strain gauge conditioner. The loads measured from the piezoelectric gauge agreed well with the AMTI load cell. The conditioner was connected

to a DAC (DASPC 3) server. The DAC server was connected to a server running VAX/VMS. A sampling rate of 5 kHz was used throughout the testing process.

All the tests were video monitored using two video cameras. These videos proved to be very helpful when analyzing the data.

4.3.4 Indentor

The indentor was a model of an *R-class* propeller blade. Only one third of the propeller blade span from the tip was manufactured. Only the suction side of the propeller blade was manufactured and the blade was strengthened on the pressure side to take the loads during high-speed indentation. The indentor was manufactured on a CNC machine at Memorial University and then polished to obtain a smooth finish at IMD.

Figure 39. Indentor Picture

The indentor was connected to the MTS machine by means of an adaptor plate machined at Tech Services, MUN. Different wedges (0°, 10°, 20°, 30°) were used in the testing process. The 0° wedge was used for pure indentation. The other wedges were used to turn the blade at small angles, which resemble the operation under small rotational speeds. This is illustrated in Figure 40.

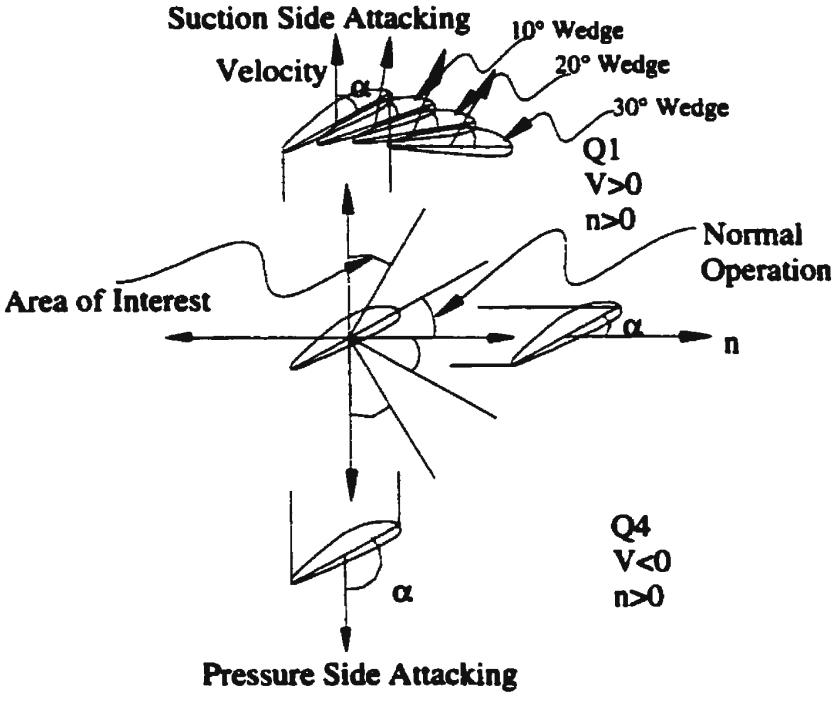

Figure 40. Indentation using wedges as opposed to normal operation

When a propeller intersects an ice piece with normal operating rotational speeds, it acts as a cutting tool, with the loads concentrating mainly at the leading edges. As the rotational speed of the propeller is decreased, the loads tend to spread more evenly along the whole chord length of the blade. During normal operating conditions (the propeller is rotating and is interacting with ice) all the blades hit the ice consecutively. But at very

slow rotational speeds, only a single blade will interact with ice, but still it is different from pure indentation. In this the blade acts as an slowly rotating indentor.

The general setup of the indentor is represented in Figure 41.

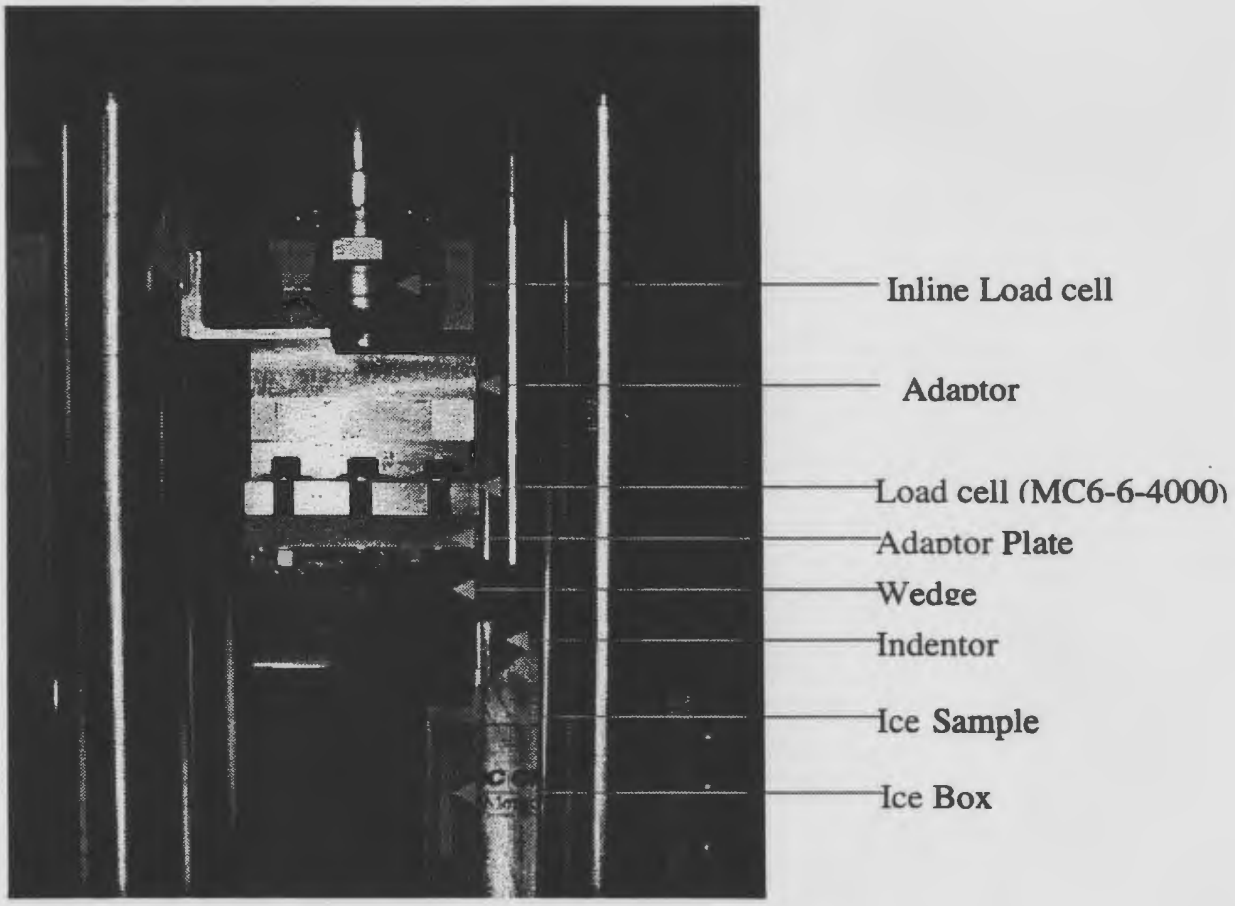

Figure 41. Indentor Setup

4.3.5 Measuring System

Measured Quantities

A measuring system employing 8 channels was used in the testing. The measured quantities were three forces (F_x, F_y, F_z), three moments (M_x, M_y, M_z), the load from the

inline piezoelectric load cell and the vertical crosshead displacement in the *z-axis* direction. All 8 channels were sampled at 5000 Hz. The full-scale deflection of the channels was ± 4V.

Calibrations

The measuring system devices were factory calibrated. The poles of the load cell were tested using a range of loads to check its operation. The values of the forces and moments obtained from the pole tests were compared with the factory calibrations. The poles were useful to check for any cross talk in the measuring system. The measuring system was checked for zeroes at the start and end of each day and also when the velocity of indentation or the wedge was changed.

4.4 Testing

4.4.1 Setup procedures

The first step in the test program was to prepare the ice block by sawing the rough-cut samples to the required dimensions (330 mm × 240 mm × 110 mm) with a chain saw. In general about 5 blocks of ice were prepared at a time. A grid was drawn on the face of the ice block with a permanent marker after the ice was cut into sample size. The grid was drawn to aid observations of ice failure during the indentation process. As the ice was placed in a box to restrain its movement, it was important to ensure that each block was the same size. The breadth of the ice block was very important because it had to be fit in

the box. After ensuring the correctness of the dimensions, the values of its dimensions were recorded and the ice block was set aside and a new block was prepared.

The ice block was fixed to the box by means of two clamps fixed to the bottom of the base plate on which the ice was placed. Wooden shims were used to adjust the ice position to maintain a constant depth of indentation.

The next step was to attach the indentor on to the appropriate wedge. The indentor was coated with toolmakers die prior to mounting. During the testing process the ink from the indentor was rubbed off from the places of contact. The area from which the ink was removed was assumed to be the contact area. The area where the die remained was assumed to be not in contact with ice. This proved very effective as similarities were observed in the contact areas when tested with the same wedge and the same velocity.

When everything in the cold room was ready the hydraulic system was turned on. The measuring system was activated and the button for the movement of the crosshead was pressed. The actual test was a fraction of a second. After the crosshead was moved to its maximum stroke, it was returned to its original position.

After the completion of the test the ice block was removed from the box and was photographed using a AGFA digital camera. For each test with a different wedge, velocity of indentation, depth of cut, a portion of the ice block was cut and stored, in labeled and sealed plastic zip bags for preparing thin sections. After this was done, the propeller was detached and was photographed to measure the contact area. Then the

toolmakers die on the indentor was wiped off using acetone and was painted again for the next test.

The final step was to analyze the collected data. Once this was done, the setup was prepared for the next test.

Some improvements were made to the test setup in the course of the test program so as to prevent turning of the indentor setup along the vertical axis. The uni-axial compressive strength of the ice was measured during a series of compression tests carried out concurrently in the large cold room.

4.4.2 Test Results

Measured forces and moments are summed and multiplied by appropriate calibration factors to give F_x, F_y, F_z and M_x, M_y, M_z. The maximum forces and moments were recorded for each test and they are analyzed for trends. The contact areas of all the tests were measured with the help of pictures taken during the testing process.

Series 1: Effect of Indentation Angle

The resultant forces and moments were plotted against the indentor angle keeping the depth of indentation constant. The velocity of indentation was 1m/s. In general it was observed that the forces and moments were insensitive to the change in angle of the indentor. As only a small range of angles of indentation were tested it was hard to predict

the trends. The plots were presented in figures 42 through 47. A lot of scatter was observed in the results for tests with same conditions. The ice failure process during the testing was not constant. Two different types of failure modes were observed. It was generally observed that whenever the ice failed by continuous crushing, the loads were high and when the ice failed by a combination of crushing and fracture, the loads were low. Each test was repeated four times to check for any trends. Even with the same input conditions such as same wedge angle, depth of indentation and velocity, the failure mode of ice was not constant. Whenever the ice has pre developed cracks, it failed by fracture and the ice without major cracks failed by crushing. It was generally observed that with low depths of indentation the ice failed by a combination of fracture and crushing and hence the wider scatter and with higher depths the ice failed by continuous crushing, hence the smaller scatter. It was observed that with the increase of the wedge angle the uncertainty of ice failure process increased.

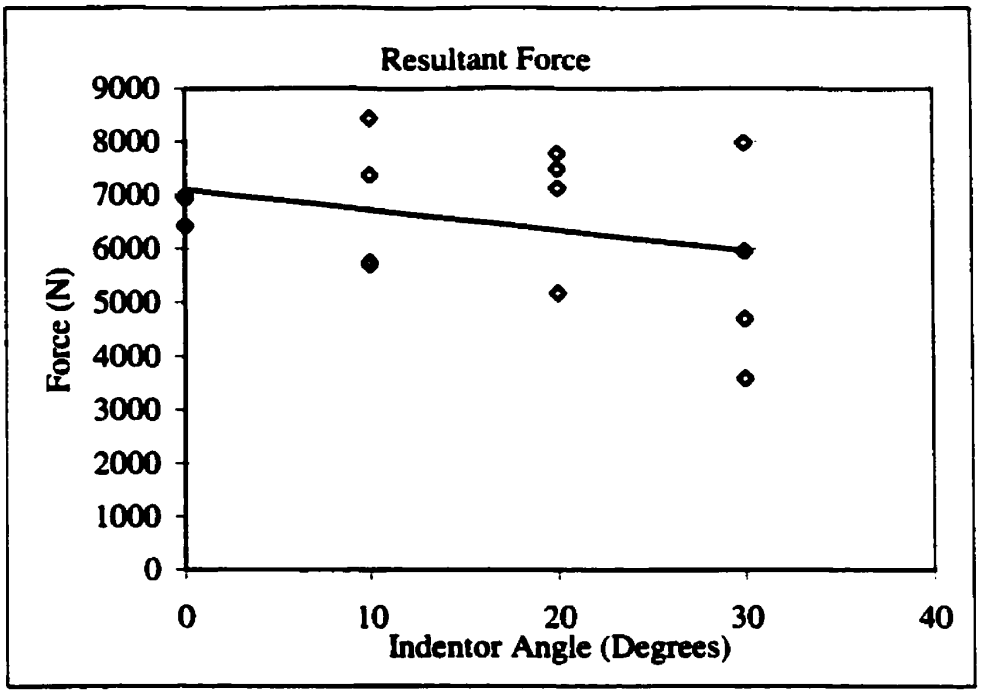

Figure 42. Resultant Force at 35 mm depth of Indentation with varying Indentor Angle

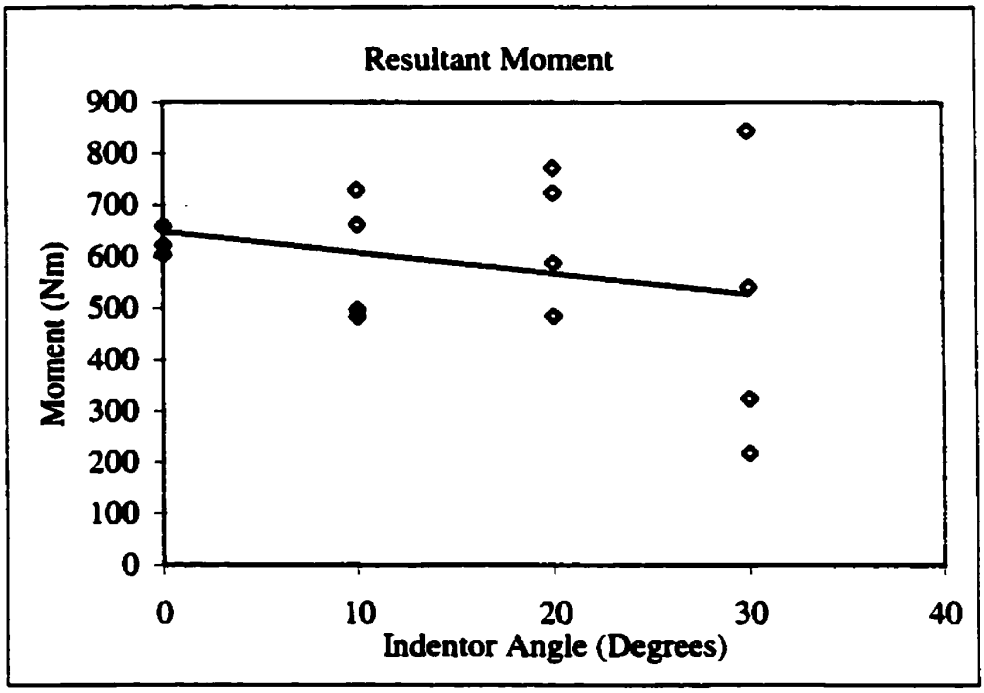

Figure 43. Resultant Moment at 35 mm depth of Indentation with varying Indentor Angle

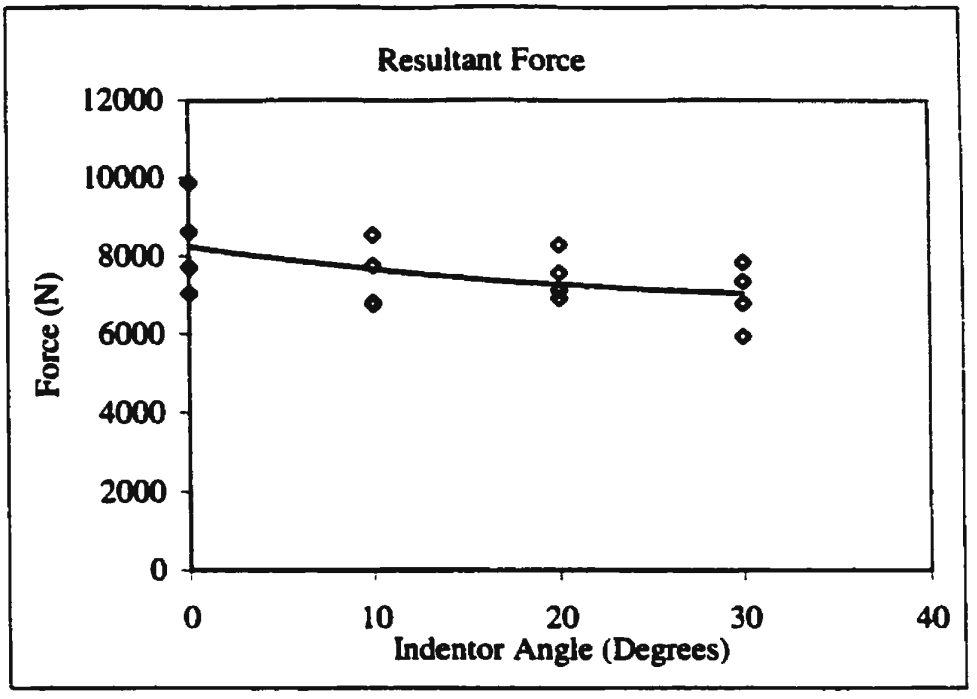

Figure 44. Resultant Force at 45 mm depth of Indentation with varying Indentor Angle

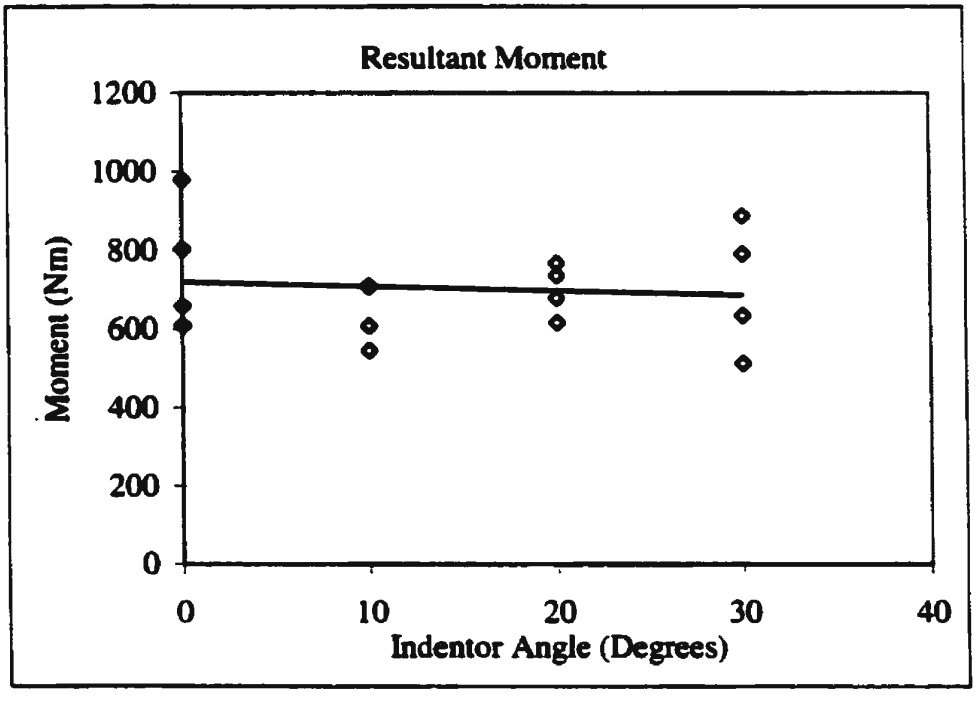

Figure 45. Resultant Moment at 45 mm depth of Indentation with varying Indentor Angle

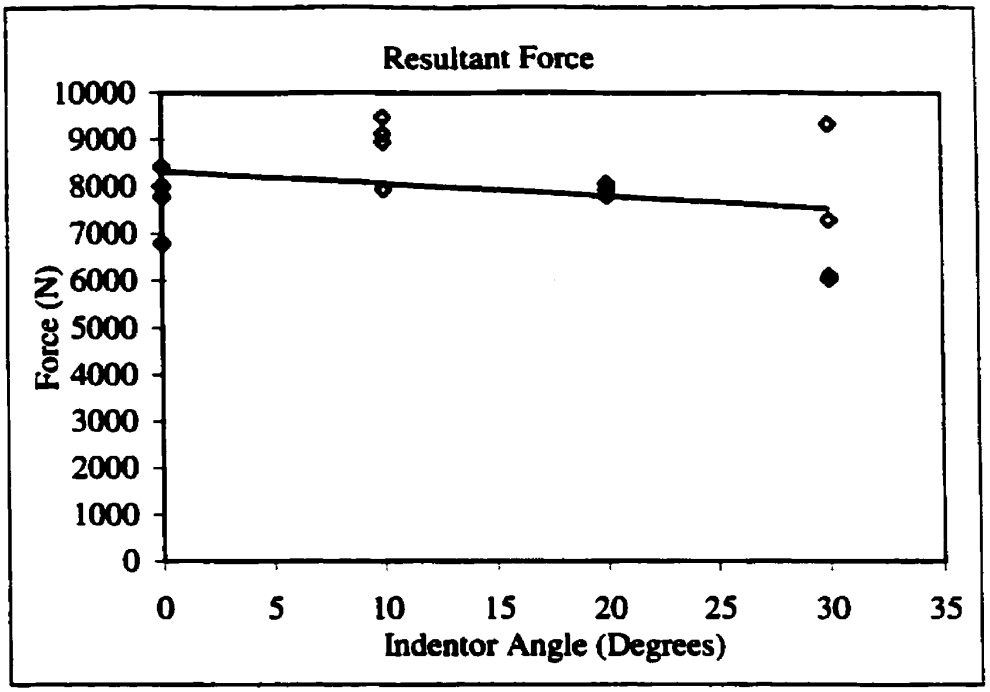

Figure 46. Resultant Force at 55 mm depth of Indentation with varying Indentor Angle

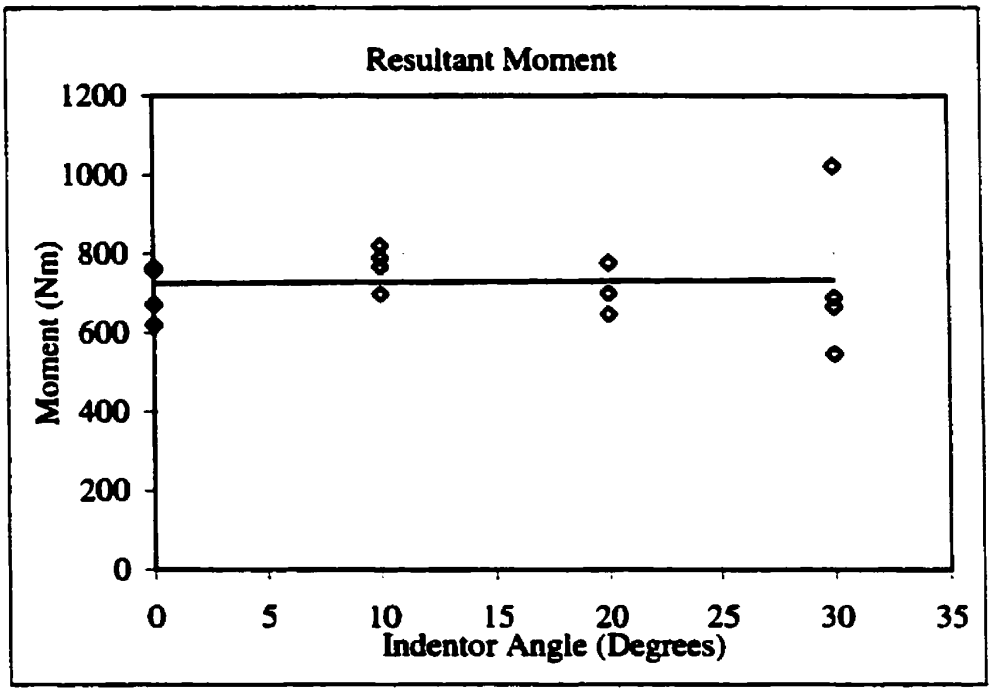

Figure 47. Resultant Moment at 55 mm depth of Indentation with varying Indentor Angle

Series 2: Effect of Indentation Speed

In this case forces and moments were plotted against velocity of indentation to check for any trends keeping the wedge angle constant at 0°. The plots are presented in Figures 48 through 53. It was observed that the forces and moments were insensitive to the velocity of indentation. As only three different velocities were tested and due to a lot of scatter in the data, it was hard to predict any trends. In general it was observed that at higher indentation speeds the scatter was minimum.

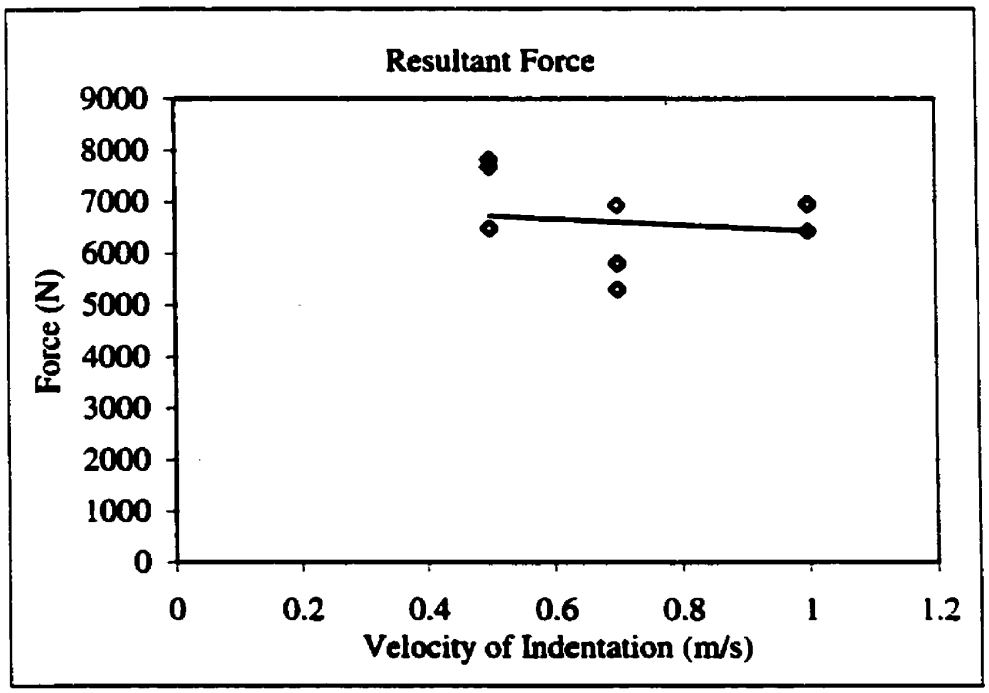

Figure 48. Resultant Force against change of velocity of indentation at 35 mm depth of indentation

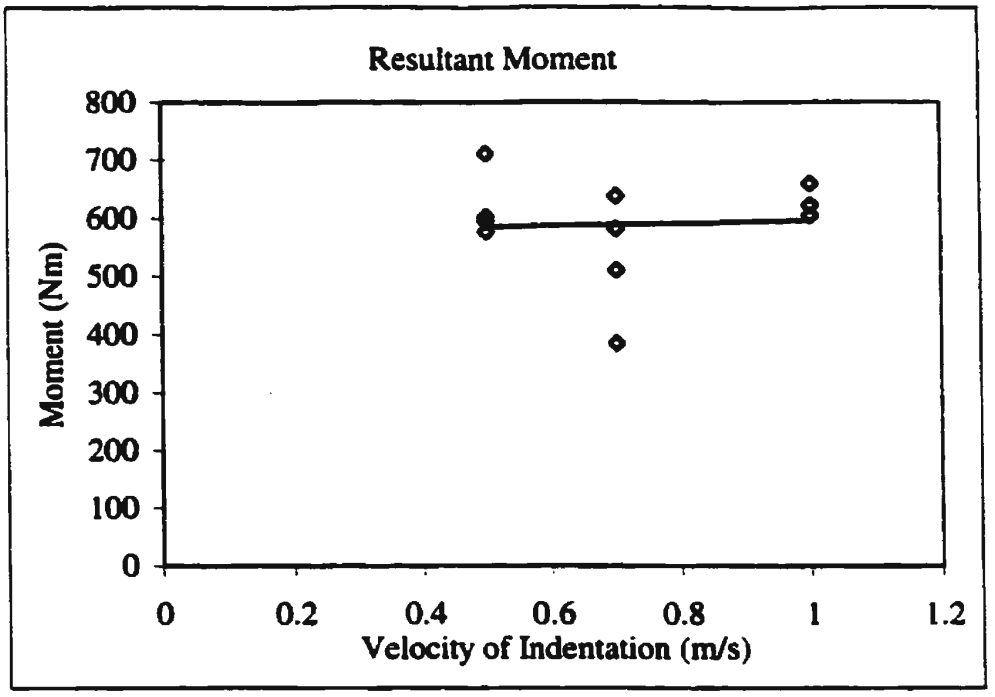

Figure 49. Resultant Moment against change of velocity of indentation at 35 mm depth of indentation

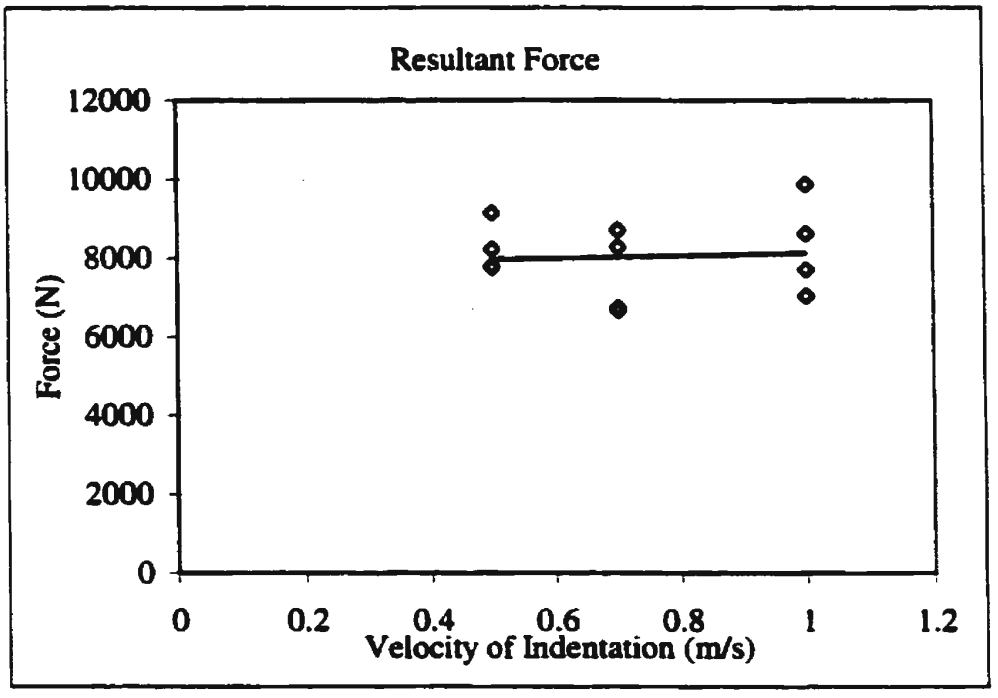

Figure 50. Resultant Force against change of velocity of indentation at 45 mm depth of indentation

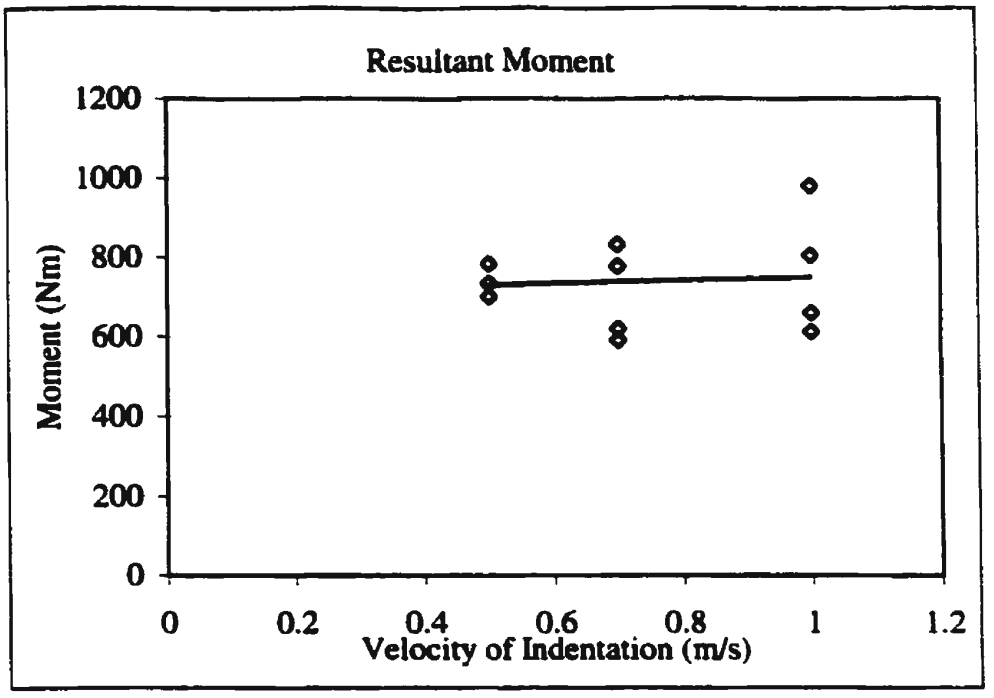

Figure 51. Resultant Moment against change of velocity of indentation at 45 mm depth of indentation

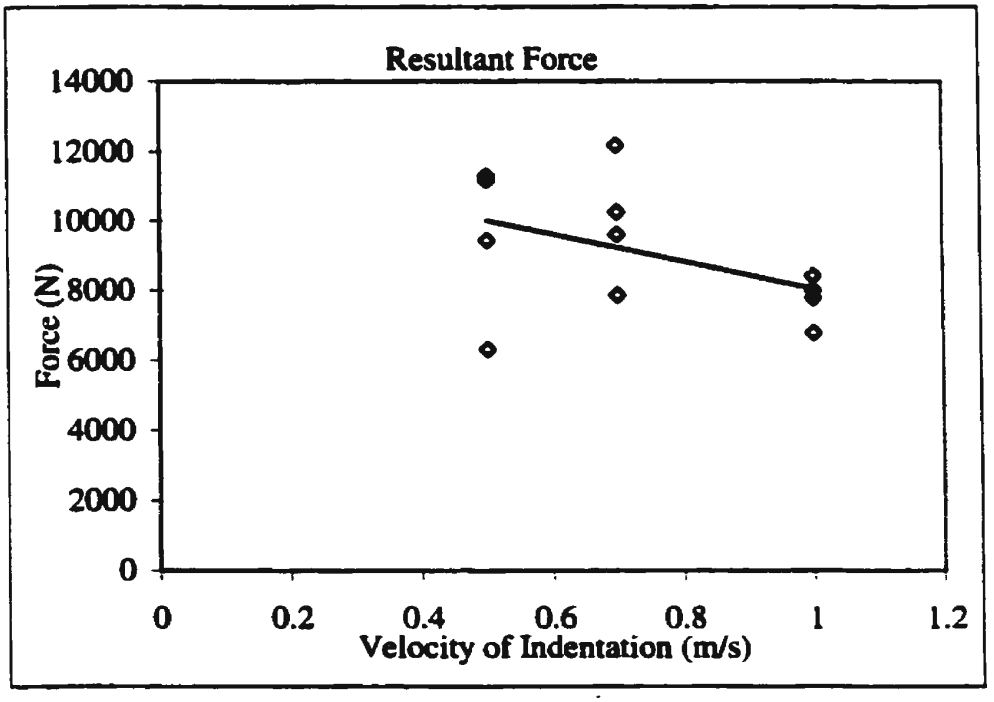

Figure 52. Resultant Force against change of velocity of indentation at 55 mm depth of indentation

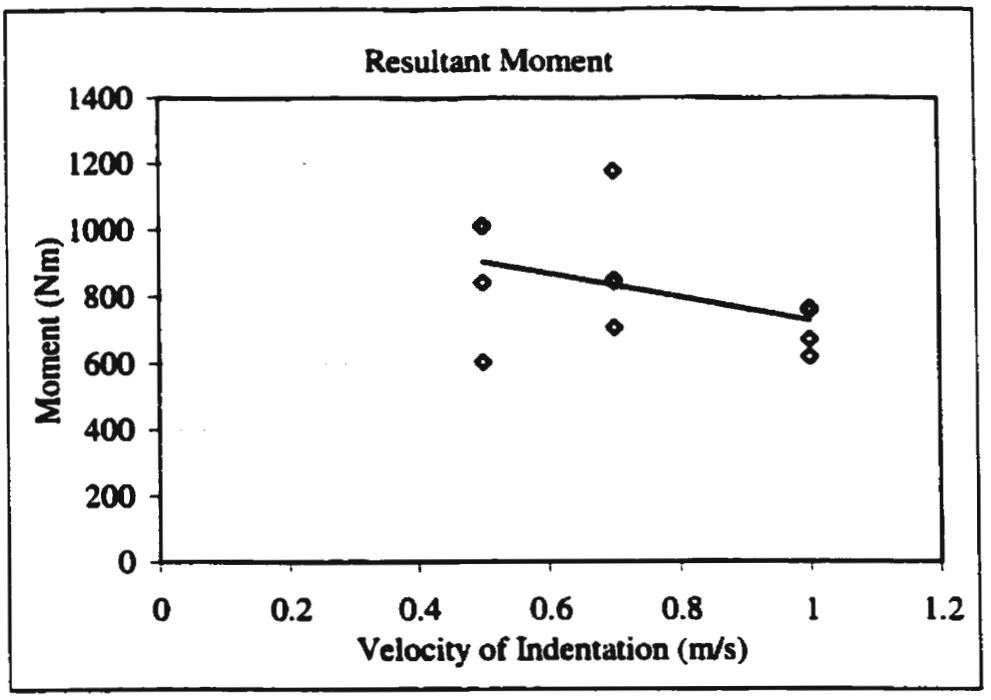

Figure 53. Resultant Moment against change of velocity of indentation at 55 mm depth of indentation

Series 3: Effect of Depth of Indentation

In this case the depth of indentation was varied and the wedge angle kept constant. It was observed that for the case of pure indentation (zero degree wedge), the depth of indentation did not affect the loads on the propeller blade, however as the indentation angle increased, the depth of indentation becomes increasingly important. In general it was observed that the loads increase with the increase of depth of indentation. As the indentation angle the scatter in the data increases due to uncertainty in the ice failure process. For zero degrees wedge, in general the ice failed by crushing. As the indentor angle was increased the mode of failure was uncertain and it caused a considerable scatter in the data. It was observed that when the mode of failure was crushing the loads were

higher and when it was fracture the loads were low. The results were presented in Figures 54 through 61.

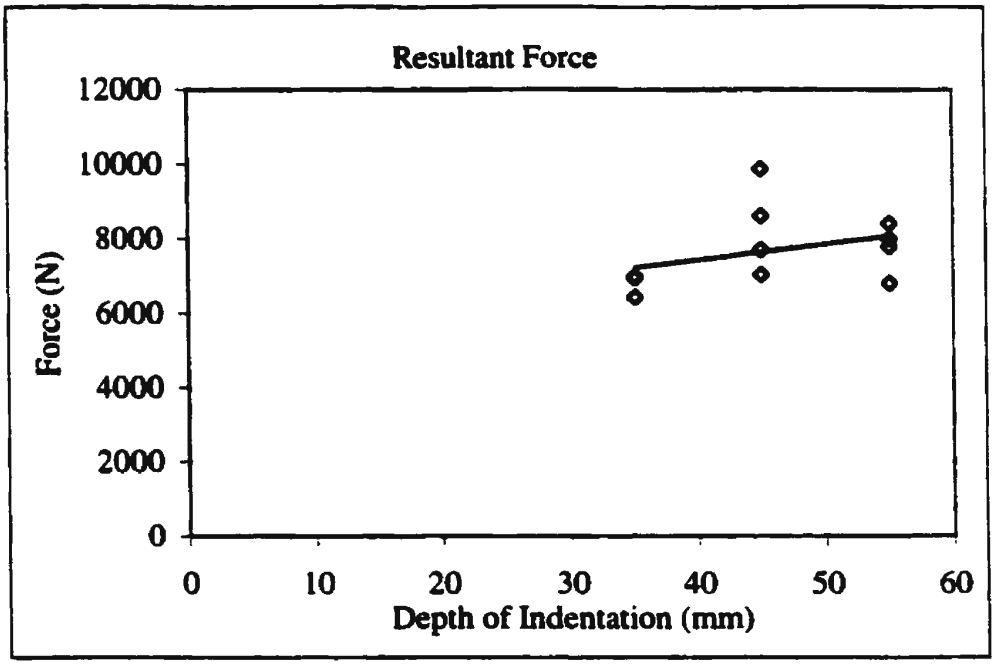

Figure 54. Resultant Force against Depth of Indentation for zero degrees Wedge

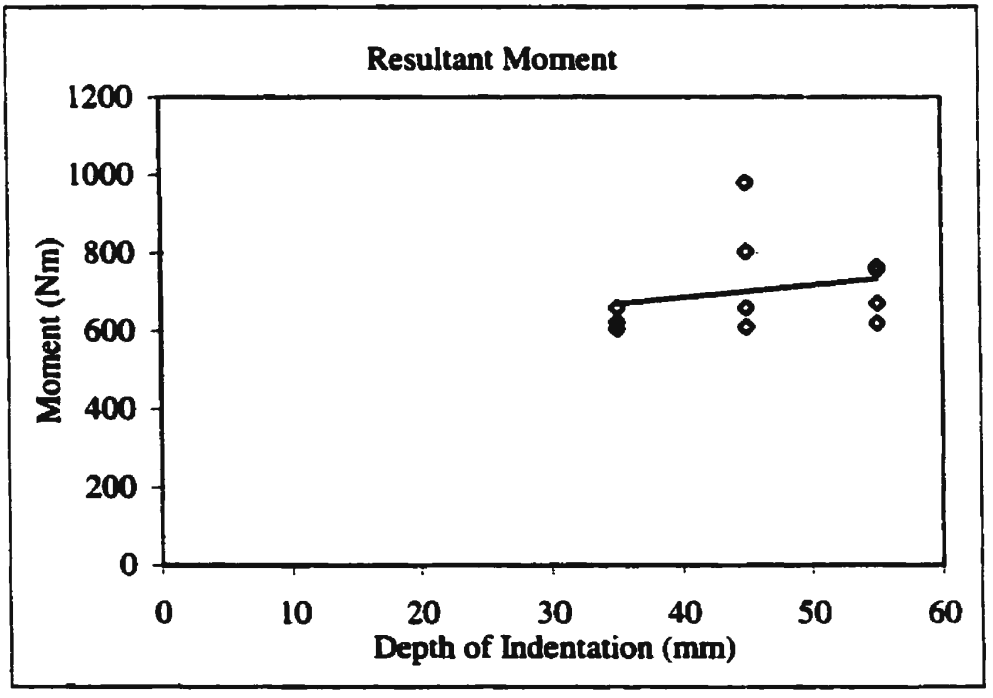

Figure 55. Resultant Moment against Depth of Indentation for zero degrees Wedge

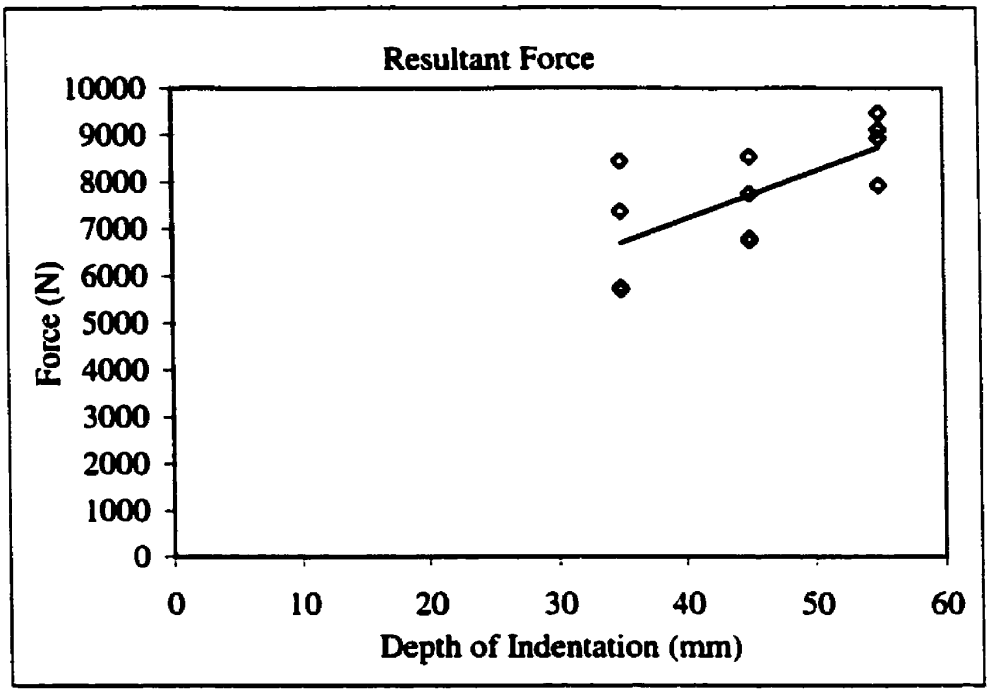

Figure 56. Resultant Force against Depth of Indentation for 10° Wedge

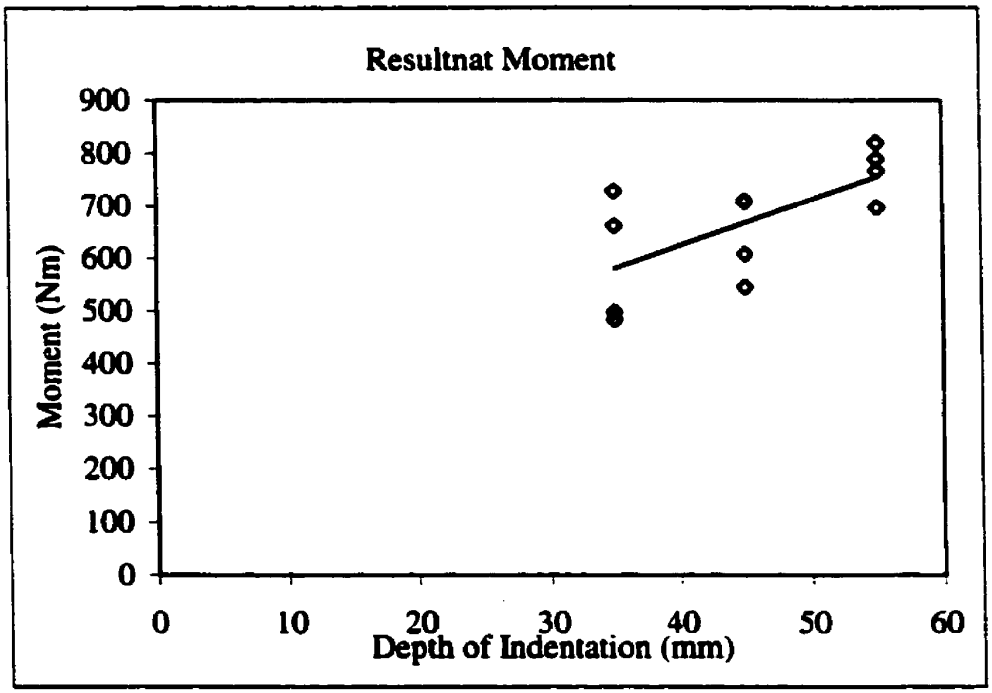

Figure 57. Resultant Moment against Depth of Indentation for 10° degrees Wedge

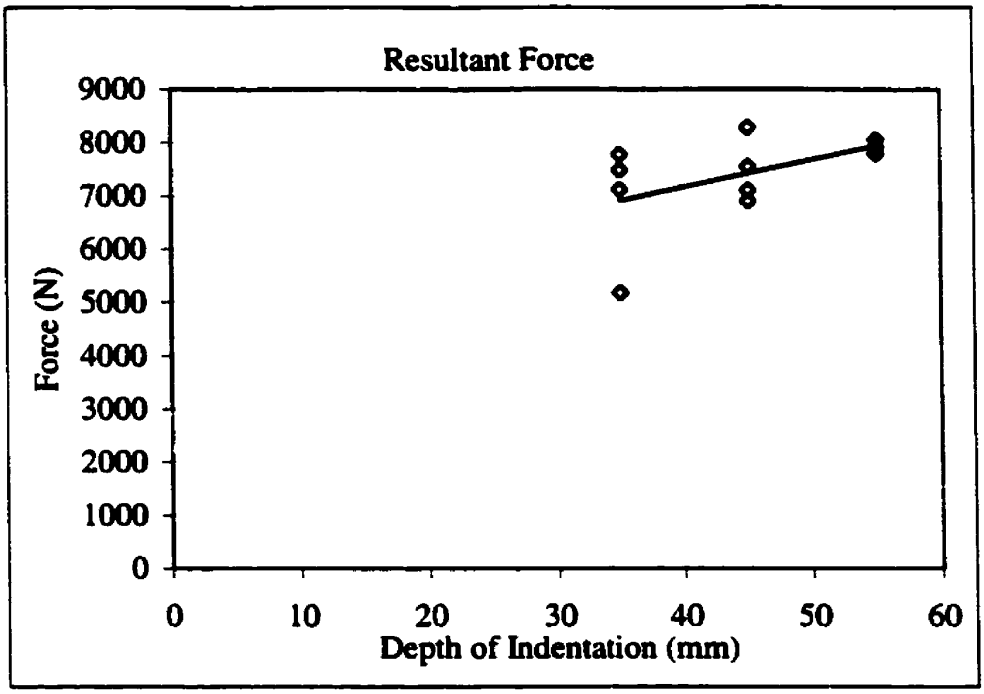

Figure 58. Resultant Force against Depth of Indentation for 20° Wedge

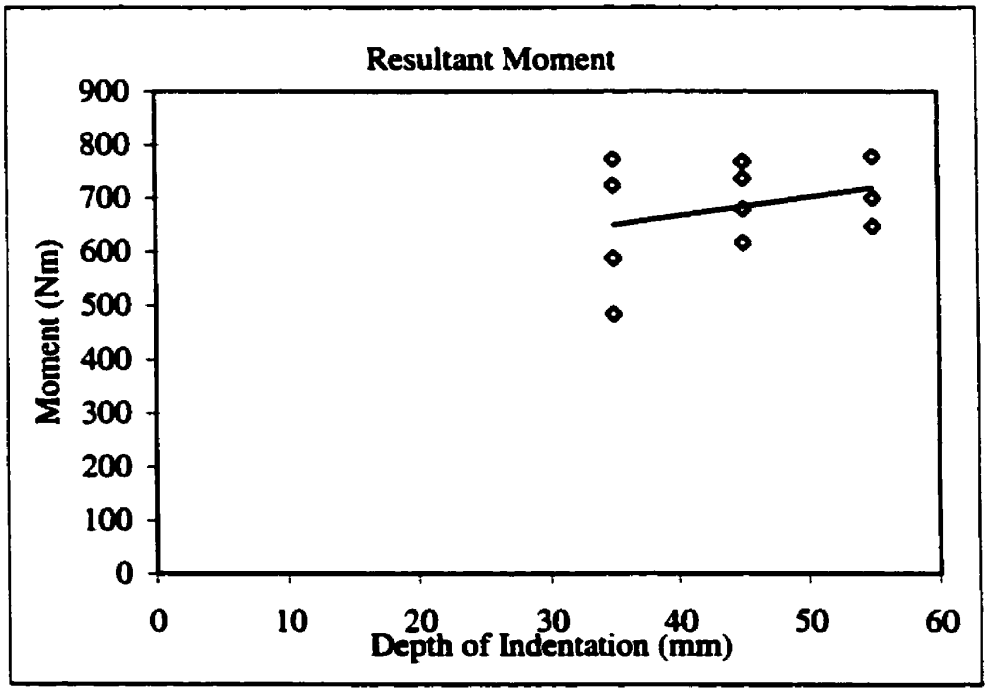

Figure 59. Resultant Moment against Depth of Indentation for 20° degrees Wedge

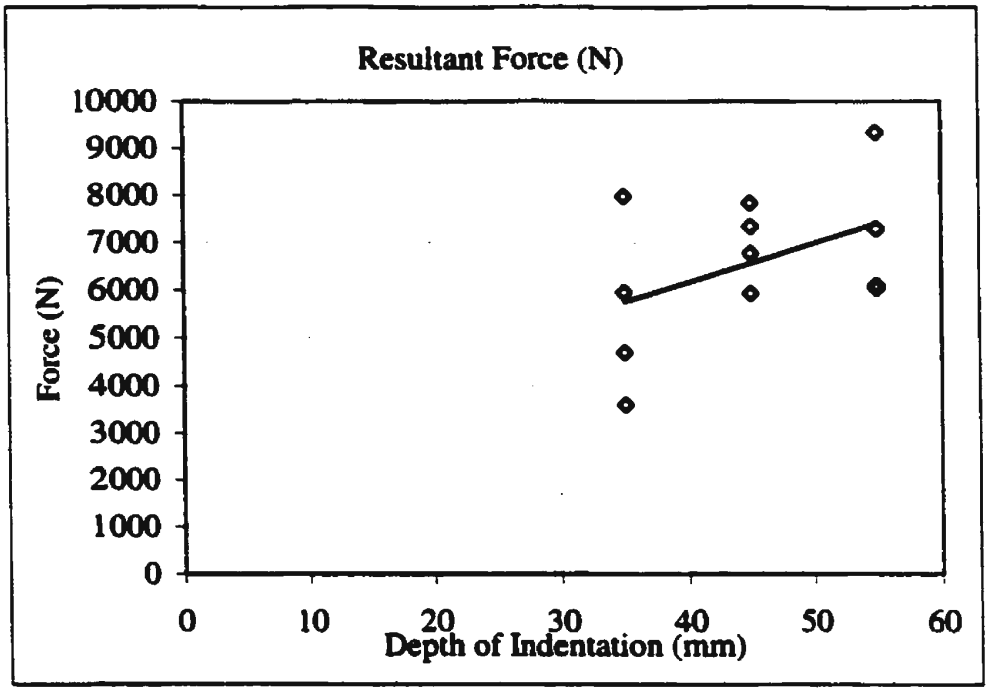

Figure 60. Resultant Force against Depth of Indentation for 30° degrees Wedge

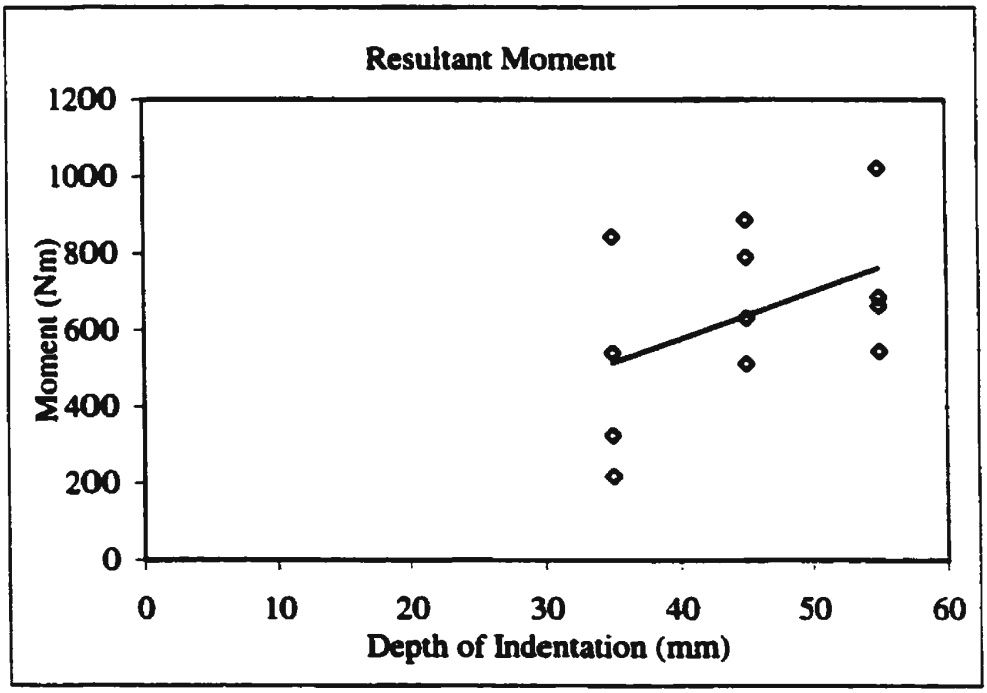

Figure 61. Resultant Moment against Depth of Indentation for 30° degrees Wedge

Contact Area Measurement and Contact Pressure

In the descriptions of the experimental procedure, it was stated that ink was sprayed onto the indentor so as to measure the nominal contact area. After the test, the ink form the portion of contact was rubbed off due to indentation process. After each test the indentor is photographed with a background of a standard scale as shown in figures 62 and 63. After all the tests were completed, the photographs of the indentor were printed and with the help of the background scale, the contact areas were measured. This was done by placing a transparency sheet on to which a graph paper is copied and measuring the squares on the transparency. where the ink was rubbed off due to indentation. The contact areas measured were used in the calculation of the contact pressures. The contact area was the area in contact while an indentor was pushed into ice. It was always less than the geometric contact area, which is the total blade surface at the given depth of indentation.

After each test the indentor is photographed with a background of standard template, which assisted in measuring the contact area. The contact areas were measured manually using a graph paper printed on a transparency sheet. The transparency sheet is laid on the picture of the indentor and the area of the indentor, which was erased due to indentation, was measured.

The ink pattern after the indentation process can be observed in Figure 62. The contact areas measured were dependent on the mode of ice failure

Figure 62. Contact Area when the ice failed by Crushing

When the ice failed by a crushing process, a continuous contact area was observed as shown in above Figure 62, while when the ice failed by fracture, contact area was not continuous but rather was patchy. An example of the contact area in patches can be observed in Figure 63.

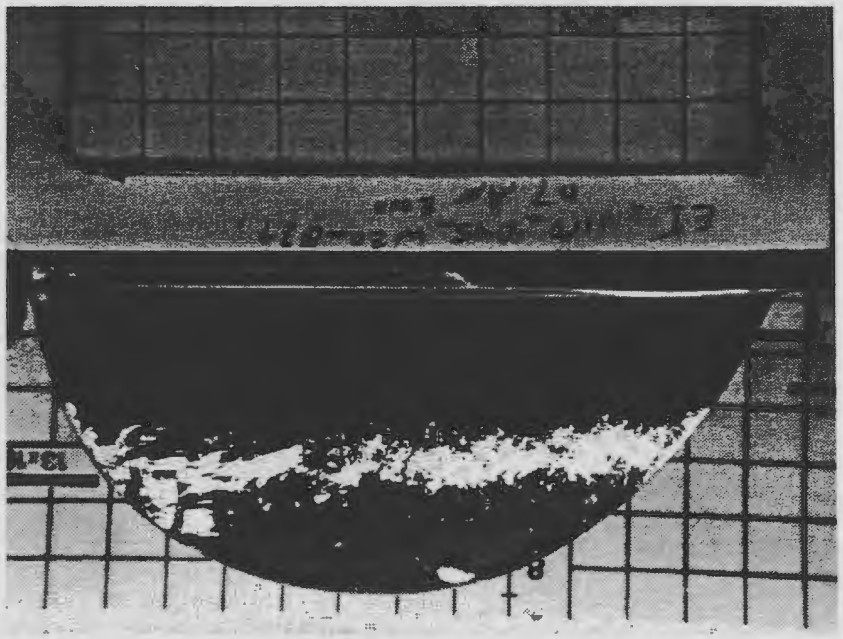

Figure 63. Contact Area when the ice failed by Fracture

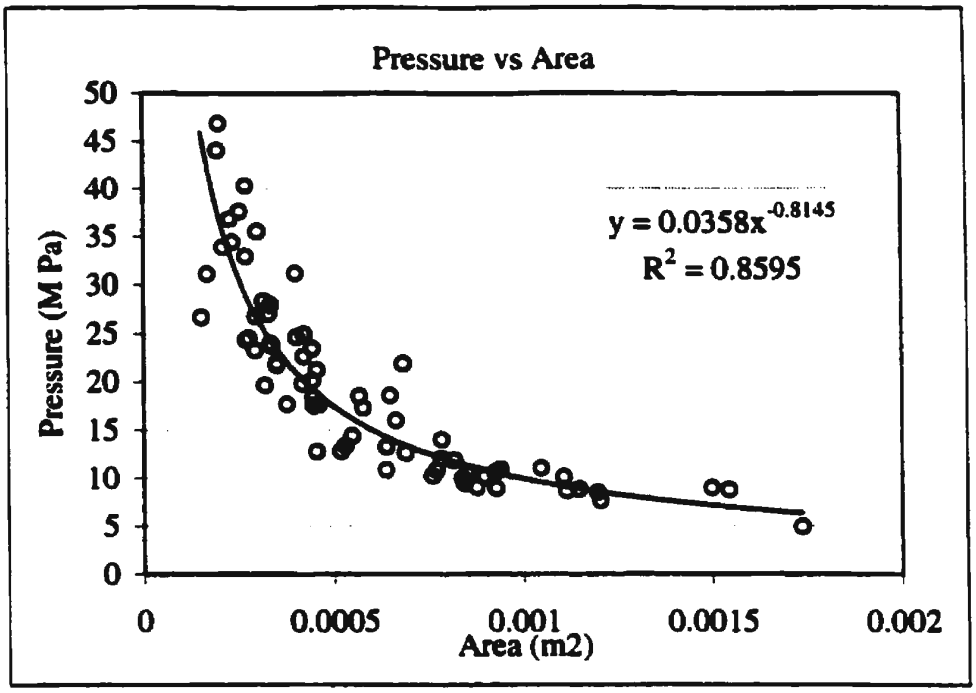

Figure 64. Contact Pressure against Contact Area

The contact pressures, which were determined by dividing the contact force by the contact area were plotted against the contact area and are shown in Figure 64. The pressures ranged between 5 and 47 MPa.

The pressures were also calculated taking into account the geometric contact area, and it was found that the pressures in this case were much smaller than the actual contact pressures. These values ranged between 0.82 and 1.98 MPa.

Chapter 5

Comparisons

5.1 Comparison of Simulation and Experimental Results

In this section the results of the experimental program and results of the simulations based on the contact model developed in Chapter 2 are compared. In addition, the propeller-ice contact model developed by Veitch (1995) for ice milling is adapted to indentation geometry and predictions made with it are compared to the experimental results and indentation contact model predictions. The simulations were done using 1:12 model scaled propeller geometry, which was same as the geometry of the propeller used in the experimental program. The input conditions (depth of indentation, velocity of indentation) were chosen to correspond to those of the experimental process.

It was observed from the experimental results that the forces and moments followed no trend at the zero degrees indentor angle, but as the indentor angle increased, the forces and moments increased with the depth of indentation. The simulations showed a linear increase of forces and moments with depth of indentation. The comparisons are presented in Figures 65 and 66. The predictions made with the model developed by Veitch (1995), although not originally intended for indentation purposes were closer to experimental results than the model developed in this thesis.

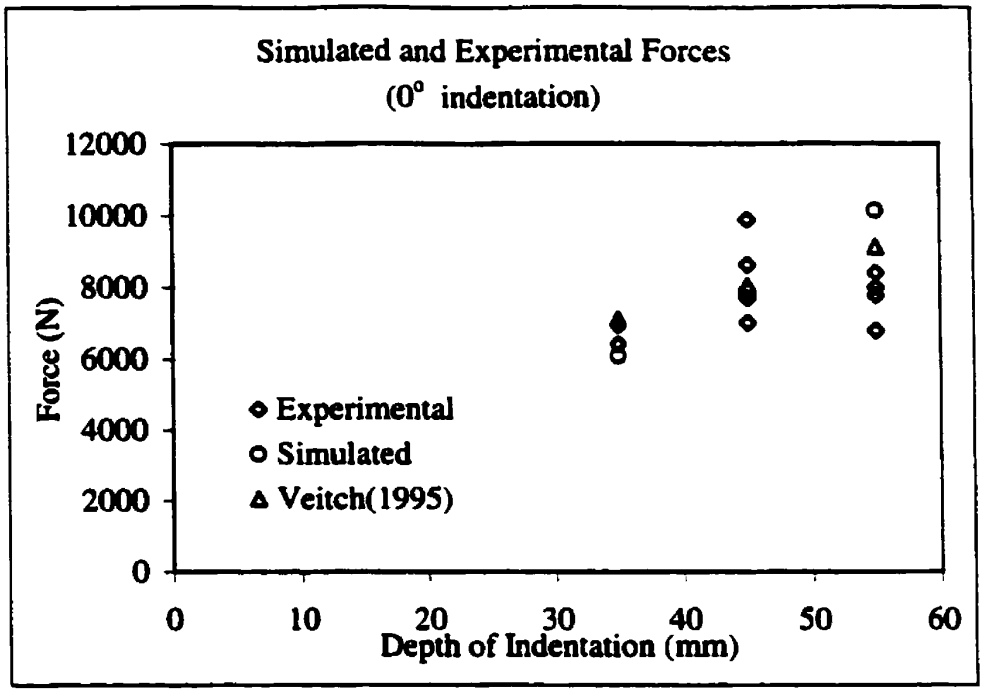

Figure 65. Simulated and Experimental Forces

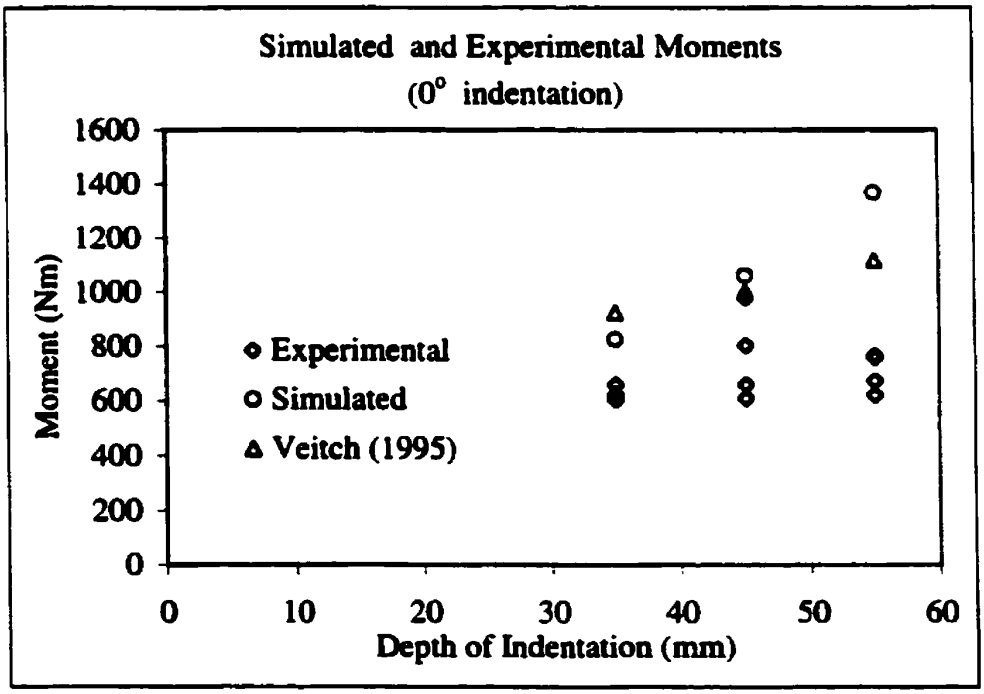

Figure 66. Simulated and Experimental Moments

One of the experimental variables was the indentor angle. A series of simulations were carried out with similar indentation angles as used in the experimental process. Sample results are shown in Figures 67 and 68. The simulations were done at 45 mm depth of indentation. A lot of scatter was observed in the experimental results. In general the forces and moments decreased with increase of wedge angle. The simulations show a constant decrease in forces and moments with increase in wedge angle.

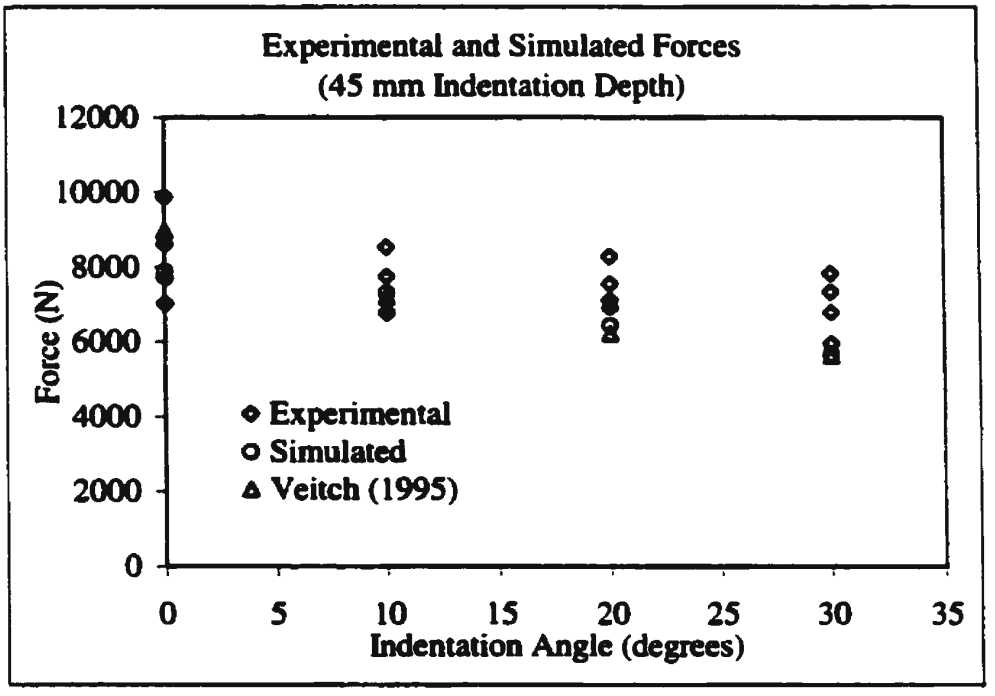

Figure 67. Experimental and simulated forces with varying indentation angles

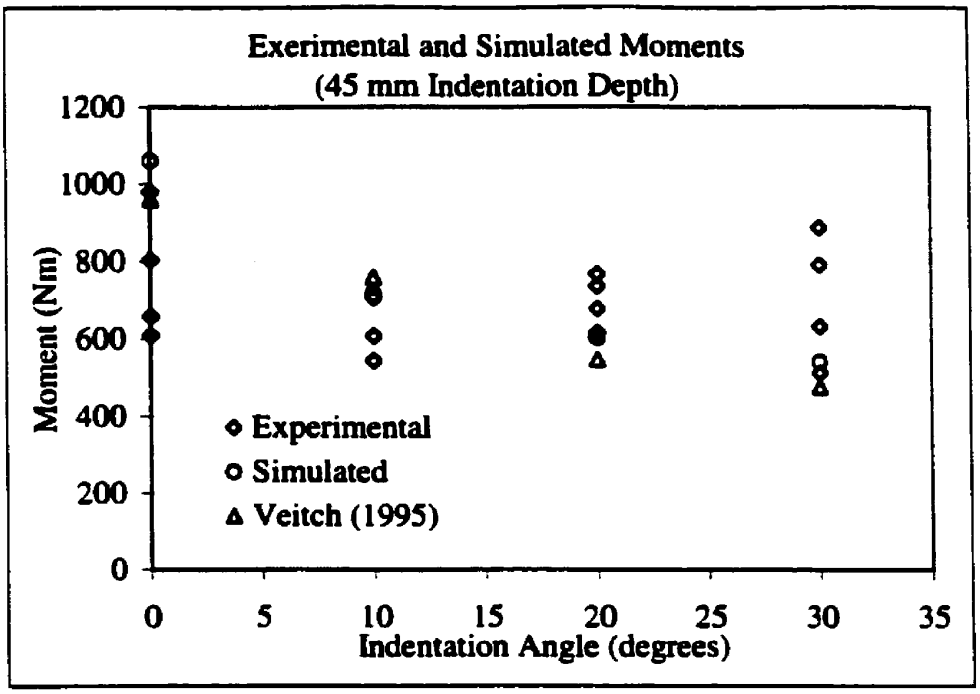

Figure 68. Experimental and simulated moments with varying indentation angles

5.2 Comparison of Contact Pressures with Bose *et al*'s (1998) Model

Jordaan *et al.* (1993) proposed an expression to calculate the pressure at a given contact area:

$$\alpha = 1.25A^{-0.70} \tag{19}$$

where A is the area of contact and α is the contact pressure. The above expression is only valid for contact areas between 0.6 and 6.0 m^2.

Taking the above expression proposed by Jordaan *et al.* into consideration, Bose *et al.* (1998) proposed an expression to calculate the extreme pressures acting on propellers with a 99% confidence interval, which can be expressed as

$$z_{0.01} = X_0 + \alpha(4.6 + \ln v + \ln r) \text{ (Jordaan } et\ al \text{ 1993)} \tag{20}$$

where X_0 is less than 0.2 between areas of 1.25 m^2 and 6.0 m^2, v is the expected number of interaction events per year and r is the proportion of events which result in pressure loading on the blade (assumed to be $1/Z_b$ or 0.25 for a propeller with four blades).

The above expression is used to calculate the design pressures over a series of contact areas and those pressures are compared with the pressures calculated from the expression proposed in Chapter 2 (taking into account 95% confidence interval, equation 6). The plot is presented in Figure 69. It can be observed that as area of contact increases the contact model developed in this thesis tends to under predict Bose *et al.*

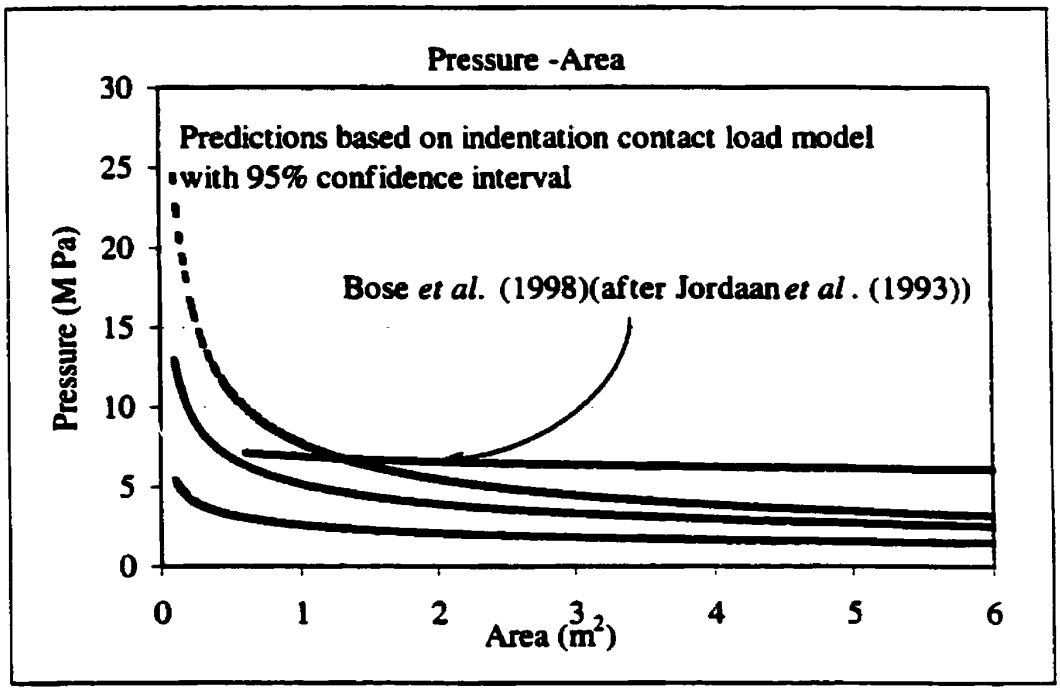

Figure 69. Comparison of Bose et al (1998) and Varma

The section modulus of the propeller (Bose *et al* 1998) blade can be calculated from the expression

$$Z_e = \gamma_{Le} \frac{M_e}{\sigma_e} \tag{21}$$

where γ_{Le} is the load safety factor, which is taken as 1.2, M_e is the bending moment and σ_e is the level of strength of the material used to resist this form of loading. As this is very exceptional loading σ_e is to be taken as ultimate tensile strength of the material.

The blade bending moment can be given as

$$M_e = \frac{P_{ice} A_E \pi D^2 (l - r_0)}{4 Z_b} \tag{22}$$

where P_{ice} is the ice pressure, A_E is the expanded blade area ratio (which is the ratio of the expanded blade area and disk area), l is the lever arm from the propeller axis to the center of pressure of the ice pressure load and Z_b is the number of blades of the propeller. The equation for the thickness of the blade at any section proposed by Bose *et al.* (1998) is

$$t = \sqrt{\frac{Z_e}{0.09 Ec}} \tag{23}$$

Here E is a constant and is taken as 1, and c is the chord length of the blade at that section.

Using Equation (23) the proposed thickness of the blade at root and at 0.6R for a series of propellers was estimated for a contact area of 2/3 of the blade area. The predictions were compared with the existing scantlings and the scantlings predicted by Bose *et al.* (1998). The predictions are given in Figures 70 and 71.

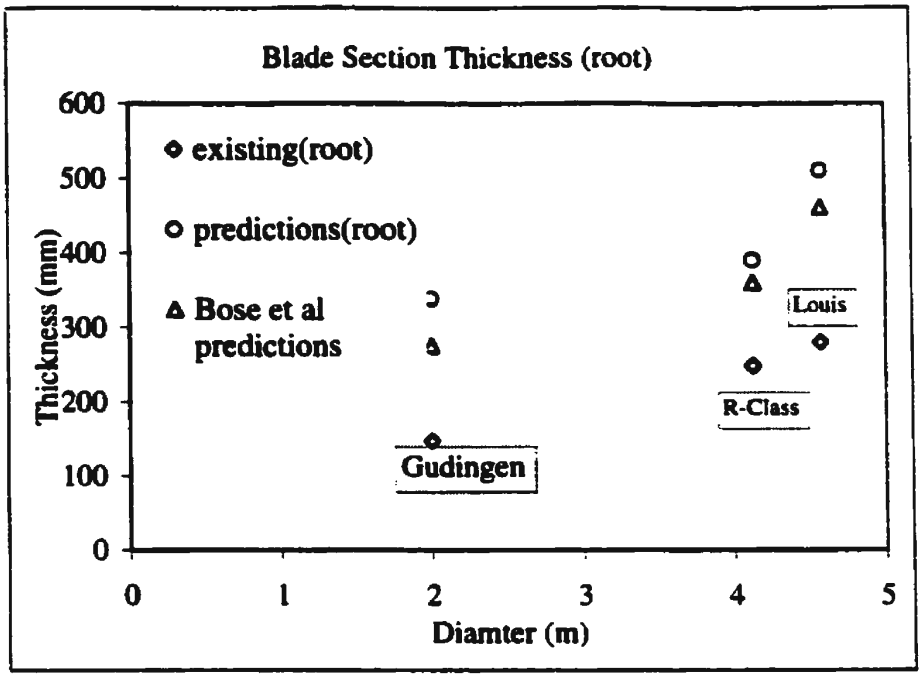

Figure 70. Proposed and existing section thicknesses at the root

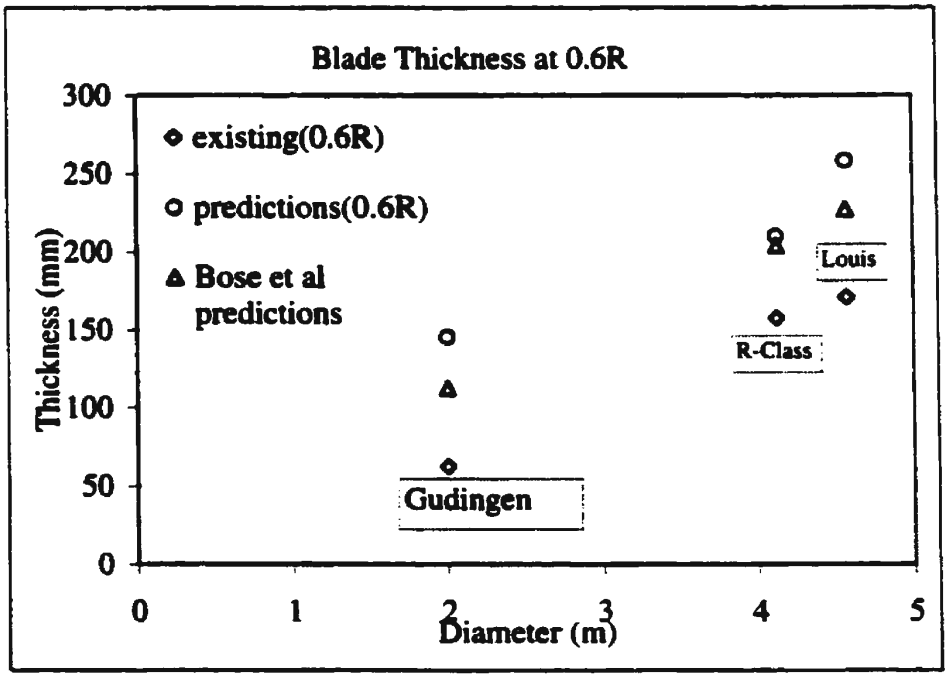

Figure 71. Proposed and existing section thicknesses at 0.6R

Chapter 6

Conclusions and Recommendations

A contact model to predict ice loads on propellers during propeller-ice indentation process was developed using the existing results of medium scale and small-scale ice-structure indentation experiments. The model, which takes the form of a pressure-area relationship, was incorporated in an existing Fortran code to simulate different loading conditions to predict ice loads on propellers. To verify the correctness of the model, a series of model scale indentation tests were performed at the Institute of Marine Dynamics using a model propeller blade and model ice. A model scale *R-class* propeller blade was used for the testing.

The results from the testing produced large scatter. This was because of the different ice failure processes observed. The main varying factors in the experimental process were depth of indentation, velocity of indentation, and indentation angle. Despite the scatter there were some discernable trends. First, the loads tended to increase with an increase in depth of indentation. The simulations carried out using the same conditions as the experimental process resulted in a linear increase in forces and moments with the corresponding increase in depth of indentation. It was observed that the measured loads were insensitive to the velocity of indentation. The predictions from the simulation model were independent of velocity of indentation, which is not included in the contact model. With the increase in the indentation angle the loads tended to decrease, but as there was also an increase in the scatter of the data with increasing wedge angle, it was hard to see

any trend. The simulated results with corresponding indentation angles produced a constant decrease in the loads with increasing indentation angle.

A series of simulations was carried out using the full-scale propeller geometry of the *R-Class* icebreaker. Two cases were considered: first with the ice fixed; then with the ice free to move. It was found that the propeller loads when operating in conditions where the ice is free to move were about 1/5 the loads predicted when the ice was fixed. This result shows that for indentation type operating scenarios, ice loads will be significantly limited if the ice pieces are free to move, or clear away from the propeller.

Simulations were also performed using the contact model developed by Veitch (1995) intended for ice milling cases. It predicted the experimental ice loads more accurately than the indentation contact model developed here. Based on various simulations done with Veitch's model, it was observed that it could be used to predict ice loads under any operating conditions.

Simulations were also carried out for different propellers. The loads for all the propellers increased linearly with the depth of indentation. However the magnitudes of the loads depended on the geometry of the propellers. It would be interesting to study the effects of rake and skew of propeller on ice loads, because the loads on different propellers behaved in a different fashion with increasing depth of indentation

The scantlings of some existing propellers were recalculated using the new indentation contact model with Bose *et al.*'s (1998) design method. The results were that the design blade thicknesses calculated with the new model were greater than the design thicknesses calculated using the original exceptional load model in Bose *et al.* (1998). Both the original and current extreme load models give design thicknesses that exceed substantially the as-designed propellers. This is not unexpected as current design practice does not treat indentation loads as a design case.

The differences in the as-designed and predicted design thicknesses raise questions regarding the practicality of designing for extreme operating scenarios. As was pointed out earlier, when ice pieces are free to move, the indentation contact loads are significantly lower than when the ice is assumed to be fixed (i.e. massive). Rather than taking the indentation between a propeller and a massive piece of ice as an extreme load design case, it would be better to base the design load case on realistic ice sizes (based upon observed piece size distributions) that are free to move, as is generally the case when navigating in ice.

REFERENCES

Belyashov, V., 1993, "An Investigation on Fracture Mechanics and Ice Loads During Cutting Fresh Water Ice by Indentors Simulating Propeller Blades", Proceedings POAC '93, Hamburg.

Belyashov, V.A. and Shapakov, V.S., 1983, "On Mechanics of Ice Crushing by propeller Blades", trans. Ice Mechanics and Physics. Nauka, Academy of Sciences of the USSR, Moscow. 10 pp

Bose, N., 1996, "Ice Blocked propeller performance Prediction Using a panel Method", Transactions of the Royal Institution of Naval Architects, Vol. 138.

Bose, N., Veitch, B., and Doucet, J.M., 1998, "A Design Approach for Ice-Class propellers", Trans. of the Society of Naval Architects and Marine Engineers.

Bose, N., Veitch, B., and Doucet, M., 1998(b), "Proposals for Design of Ice-Class propellers", TP 13213E, Transportation Development Center.

Bulat, V., Majid, I., and Goosens, L., 1985, "Experimental Determination of Factors Affecting Loads Imposed on Propellers in Ice", Transport Canada Publication TP 6812E.

Chernuka, M.W., Jategaonkar, R.P., Norwood, M.E., and Warner, J.L., 1989, "Development of a Procedure for Predicting Propeller-Ice Interaction Forces", Transport Canada Publication TP 9850E.

Conrad, N., 1976, "On Microcrack Growth and Arrest in Simulated Fibrous Composites", Mechanics and Materials Research Center, Texas A&M Univesrity, College Station, Report MM 3168-76-10.

Cottrel, B. and Rice, J.R., 1980, "Slightly Curved or Kinked Cracks", International Journal of Fracture Mechanics, Vol. 16, pp.155-169.

Daley, C., 1994, "Compilation of Medium Scale Ice Indentation Test Results and Comparison to ASPPR", Transport Canada Publication TP 12151E.

Defranco, S.J. and Dempsey, J.P., 1990, "Crack Growth Stability in S2 Ice", IAHR Ice Symposium, Espoo, Finland.

Duff, J., Kirby, K., and Laskow, V., 1985, "Measurement of Ice-Propeller Interaction Parameters:M. V. Robert Lemeur: Main Report", Transport Canada Publication TP 6839E.

Edwards, R.Y., 1976, "Methods for Predicting Forces Encountered by Propellers During Interactions with Ice", Intl. Shipbuilding Progress, Vol. 23, No. 268.

Enkvist, E., and Johansson, B.M., 1968, "On Icebreaker Screw Design", European Shipbuilding, Vol. 16, No. 1, Oslo.

Eranti, E., 1990, "Numerical Simulation of Dynamic Ice Structure Interaction" Proceedings 10th IAHR Symposium on Ice, Espoo, Finland, Vol. 2 pp. 912-922.

Evans, A.G., Palmer, A.C., Goodman, D.J., Asbhy, M.F., Hutchinson, J.W., Ponter, A.R.S. and Williams, G.J., 1984, "Indentation Spalling of Edge-loaded Ice Sheet", IAHR Ice Symposium, Hamburg.

Frederking, R., Jordaan, I.J., Mccallum, J.S., 1990, "Field Tests of Ice Indentation of Medium Scale Hobson's Choice Ice Island, 1989" Proceedings 10th IAHR Symposium on Ice, Espoo, Finland, Vol 2, pp. 931-944.

Frederking, R.M.W., Jordaan, I.J., and Mccallum, J.S., 1990, "Field Test of Ice Indentation at Medium Scale, Hobson's Choice Ice Island", Proceedings of 10th IAHR Symposium on Ice, Espoo, Finland, Vol. 2, pp. 931-944.

Gabel, D.G., Parsons, M.G., kaldjian, M.J., 1979, "Finite Element Structural Analysis for Displacements Occurring in the Hub of a Polar Class Icebreaker Controllable Pitch Propeller Operating in Ice", Department of Naval Architecture and Marine Engineering Report No. 217, The University of Michigan.

Glen, I.F. and Blount, H., 1984, "Measurement of Ice Impact Pressure and LoadsOnboard CCGS Louis S. St. Laurent", Offshore mechanics and Arctic Engineering Symposium, New Orleans, Vol III, pp. 246-252.

Hutchinson, J.W. and Suo, Z., 1992, "Mixed Mode Cracking Layered Materials", **Advances in Applied Mechanics,** Academic Press, Vol 29, pp. 63-191.

Ignatjev, M.A., 1964, "Determination of Ice Loads Encountered by Ship Propeller Blades", Trans. Problems of the Arctic and Antarctic, No. 15, pp. 41-51.

Ignatjev, M.A., 1966, "Screw propellers for Ships Navigating in Ice", Trans. Sudostroenie.

IITC, 1978, "Report of the Resistance and Flow Committee", 15th International towing Tank Conference, Ottawa, Canada.

Jagodkin, V.Y., 1963, "Analytical Determination of the Resistance Moment of a Propeller During its Interaction with Ice", Trans. Problems of the Arctic and Antarctic, Vol. 12,pp. 78-88.

Joensuu, A., and Riska, k., 1988, "Contact Between Ice and Structure", Helsinki University of Technology, Laboratory of Naval Architecture and Marine Engineering. Report M-88. Otaniemi.

Jussila, M., 1983, "Ice Loads on the Propulsion System of an Icebreaking Tug", POAC '83, Espoo, Finland.

Jussila, M., and Koskinen, P., 1989a, "Ice Loads on CP-Propeller Shaft of small Ferry and their Statistical Distributions during Winter '87", OMAE, The Hague.

Jussila, M., and Koskinen, P., 1989b, "Ice Loads on Propeller Blade of Small Car Ferry", POAC '89 Vol. 2, Lule.

Jussila, M., and Soininen, H., (1991), "Interaction between Ice and propeller", Research Notes 1281, Technical Research Center of Finland, Espoo.

Kannari, P., 1988, "Full Scale and Model Tests Performed with a Nozzle and Open Propeller Simultaniously", IAHR Symposium, Sapporo.

Karna, T., and Muhonen, A., 1990, "Preliminary Results from Ice Indentation Tests Using Flexible and Rigid Indentors", IAHR Ice Symposium, Espoo, Finland, Vol. 3, pp.261-275.

Karna, T., and Muhonen, A., 1990, "Preliminary Results from Ice Indentation Test using Flexible and Rigid Indentors" Proceedings 10th IAHR Symposium on Ice, Espoo, Finland, Vol. 3, pp. 261-275.

Katzmann, F.M., and Andriushin, A.V., 1997, Strength Rates for Blades as Intended for the Propellers of Ice-Breakers and Ice Ships", Russian Maritime Register of Shipping.

Keinonen, A.J., and Browne, R.P., 1990, "Ice Propeller Interaction Forces", Transport Canada Publication 10401E Vol. 1.

Kendall,K., 1978, "Complexities of Compression Failure", Proceedings of the Royal Society of London, Vol. A361, 1978, pp. 245-263.

Korzhavin, K.N., 1962, "Action of Ice on Engineering Structures. USSR Acad of Sci. Siberian Branch. CRREL Draft Translation No. 260, Hanover, USA, 1971.

Koskikivi, J., and Kujala, P., 1985, "Long Term Measurements of Ice Induced Loads on the Propulsion Machinery of Product Tanker Sotka", Winter Navigation Research Board Report No. 42, Finnish Board of Navigation.

Kotras, T., Humphreys, D., Baird, A., Morris, G., and Morley, G., 1985, "Determination of Propeller-Ice Milling Loads", OMAE '85, Dallas, Vol. 2 pp. 336-343.

Lindroos, H., and Bjorkestam, H., 1986, "Hydrodynamic Loads Developing During Ice-Clogging of a Propeller Nozzle and Means to Prevent Clogging", PolarTech '86 International Offshore and Navigation Conference and Exhibition, Vol. 2, Technical Research Center of Finland, Espoo.

Liu, P., 1998, "A Time Domain Panel Method for Oscillating Propulsors with Both Chordwise and Spanwise Flexibility", Ph.D. Doctoral Thesis, Memorial University of Newfoundland, St.John's, Canada.

Maes., M.A., Jordaan, I.J. and Cormeau, A., 1986, " Probabilistic Theories For the Failure of Sea Ice", International conference on Ice Technology, MIT, Boston, pp. 37-54.

Newbury, S., Shih, L.Y., Browne, R.P., Revill, C.R., Kenny, S., and Zheng, Y., 1993, "Experimental and Theoretical Evaluation of Hydrodynamic Pressure During Non-Contact Propeller-Ice Interaction", Proceedings of the 2nd Canadian Marine Conference, Vancouver.

Okamoto, H., Nozawa, K., Kawakami, H., Yamamoto, F., 1981c, "Dynamic Ice Loads and Stress Analysis on the Propeller of the Arctic Ship; Model Test in Ice", POAC '81, Vol. 1, Quebec.

Okamoto, H., Shimoyama, N., Yamamoto, F., Nozawa, K., Iijuka, K., and Matsumura, H., 1981a, "Experimental Study on Propeller Ice interaction for Icebreaking Merchant Ship, 1st Report: Ice Load Model Experiments", Journal of the Society of Naval Architects of Japan, Vol. 149, No. 4.

Okamoto, H., Shimoyama, N., Yamamoto, F., Nozawa, K., Iijuka, K., and Matsumura, H., 1981b, "Experimental Study on Propeller Ice interaction for Icebreaking Merchant Ship, 2nd Report: Static Load Test and FEM Analysis", Journal of the Society of Naval Architects of Japan, vol. 150, No. 4.

Palaniswamy, P. and Knauss, W.G., 1974, "On the Problem of Crack Extension in Brittle Solids Under general Loading", California Institute of Technology, SM-74-8.

Palmer, A.C., and Sanderson, T.J.O., 1991, "Fractal crushing of Ice and Brittle solids", Proceedings of royal Society of London, Ser. A 433, 469-477.

Riska, K., Rantala, H., and Joensuu, A., 1990, "Full Scale Observations of Ship- Ice Contact", Helsinki University of Technology, Laboratory of Naval Architecture and Marine Engineering. Report M-97.

Saeki, H., and Ozaki, A., 1980, "Ice Forces on Piles" Physics and Mechanics of Ice, Springer-Verlag, pp. 342-350.

Saeki, H., Hirayama, K.I., Kawasaki, T., Akagawa, S., Kato, K., Kamesaki, K., Saka, K., and Kurokawa, A., 1996, "JOIA Project of study of Ice Load" Proceedings 13th International Symposium on Ice, Beijing, China, Vol. II, pp. 785-811.

Sasajima, T., 1985, "Ice Milling Loads encountered by a Controllable Pitch Propeller", Mitsubishi Technical Bulletin No. 170, Mitsubishi Heavy Industries Ltd., Tokyo.

Sasajima, T., and Mustamaki, E., 1984, "Ice Milling Loads Encountered by a Controllable Pitch Propeller", IAHR Ice Symposium, Hamburg.

Sasajima, T., Bulat, V., and Glen, I., 1981, "An Experimental Investigation of two Candidate Propeller Designs for Ice Capable Vessels", POAC '81, Vol. 1.

Searle, S., 1999, "Ice Tank Tests of a Highly Skewed Propeller and a Conventional Ice-Class Propeller in Four Quadrants", M. Eng Thesis, Memorial University of Newfoundland.

Shih, L.Y., and Zheng, Y., 1992, "Constricted Hydrodynamic flow due to Proximate Ice Blockage over a Blade Profile in Two Dimensions", Proceedings 2nd international Symposium on Propellers and Cavitation, Hongzou.

Shih, L.Y., and Zheng, Y., 1993, "Application of 3-D BEM to Time dependent Potential Flow Around a Propeller Blade Profile Suring Ice Contact", Proceedings International shipbuilding Conference, St. Petersburg.

Sih, G.C. and Tzou, D.Y., 1983, "Mechanics of Nonlinear Crack Growth: Effects of Specimen Size and Loading Steps", Conference on Modeling Problems in Crack Tip Mechanics.

Sih, G.C., 1973, "A Special Theory of Crack Propagation", in Mechanics of Fracture 1, Methods and Analysis and Solutions and Crack Problems, Ed. G.C. Sih, Nordoff, Leyden, pp. XXI-XLV.

Sodhi, D.S., 1991, "Ice Structure Interaction During Indentation Tests" Proceedings of IUTAM-IAHR Symposium. Springer-Verlag, Berlin, pp. 619-640.

Sodhi, D.S., 1992, "Ice Structure Interaction with Segmented Indentors" Proceedings 11th
IAHR Symposium on Ice 1992, Banff, Alberta, Canada, Vol. 2, pp. 909-929.

Sodhi, D.S., 1998, "Non-simultaneous Crushing During Edge Indentation of Fresh Water Ice Sheets", Cold regions Science and Technology, 27 pp. 179-195.

Sodhi, D.S., Takeuchi, T., Nakazawa, N., Akagawa, S., and Saeki, H., 1998, "Medium Scale Indentation tests on Sea Ice at various Speeds", Cold Regions Science and Technology 28(1998) pp. 161-182.

Soininen, H., Jussila, M., Koskinen, P., Jones, S.J., Newbury, S., and Browne, R., 1997, "Propeller-Ice Interaction", Transactions of the society of Naval Architects and Marine Engineers, Vol. 105. pp. 399-425

Soininen, H., Liukkonen, S., and Muhonen, A., 1995, "Laboratory Tests of propeller Blade Profile Pressure Distribution under Ice Contact", Research Notes 1664, technical Research Center of Finland, Espoo. 127pp.

Tamura, K., Kato, H., and Yamaguchi, H., 1997, "Experimental Approach to the Interaction between Nozzle-Propeller and Ice Block", Joint OMAE/POAC Conference, Yokohama, Japan.

Timco, G.W., 1986, "Indentation and Penetration of Edge Loaded Fresh Water Ice Sheets in the Brittle Range", Proceedings 5th OMAE, Tokyo.

Tuhkuri, J., 1994, "Analysis of Ice Fragmentation Process from Measured Particle size Distributions of Crushed Ice" Cold regions Science and Technology. 23, 69-82.

Tuhkuri, J., 1995, "Experimental Observations of Brittle Failure Process of Ice and Ice-Structure Contact" Cold Regions Science and Technology. 23, 265-278

Tuhkuri, J., 1996, "Experimental Investigations and Computational Fracture Mechanics Modelling of Brittle Ice Fragmentation", Acta Polytechnica Scandinavica, Mechanical Engineering Series No. 120. Helsinki, 105 pp.

Veitch, B., 1995, "Predictions of Ice Contact Forces on a Marine Screw Propeller During the Propeller-Ice Cutting process", Acta Polytechnica Scandinavica, Mechanical Engineering Series No. 118. Helsinki, 140 pp.

Veitch, B., 1992, "Propeller-ice Interaction", Licentiate of technology Thesis, Helsinki University of Technology, Espoo.

Veitch, B. 1994. Results of ice cutting experiments with cutting tools representing propeller blade sections. *Proc. IAHR Ice Symposium*, Trondheim, pp.886-895.

Veitch, B., and Kivela, J., 1993, "Results of Ice Cutting Experiments with Cutting Tools Representing Propeller Blade Sections", Report M-183, Ship Laboratory, Helsinki University of Technology, Espoo.

Veitch, B., Bose, N., Jordaan, I.J., Haddara, Md., and Spencer, D., 1999, "Ice Capable Ships", Sname Ship Design and Construction Revision Chapter No 33.

Walker, D., and Bose, N., 1994b, "Hydrodynamic Performance and Cavitation of an Open Propeller in a Simulated Ice Blocked Flow", Proceedings of Propeller/Shafting '94, Virginia Beach, Paper No. 20.

Walker, D., Bose, N., and Casey, S., 1994c, "Ducted Propeller Cavitation in Blocked Flow", 2nd International Symposium on Cavitation, Tokyo.

Walker, D., Bose, N., and Yamaguchi, H., 1994a, "Hydrodynamic Performance and Cavitation of an Open Propeller in a Simulated Ice Blocked Flow", Journal of OMAE, Vol. 116.

Walker, D.L.N., 1996, "The Influence of Blockage and Cavitation on the Hydrodynamic Performance of Ice Class propellers in Blocked Flow", Ph.D. Doctoral Thesis, Memorial University of Newfoundland, St.John's, Newfoundland, Canada.

Wind, J., 1983, "The Dimensioning of High Power propeller System for Arctic Icebreaking Vessels", Proceedings, The 5th Lips Propeller Symposium.

Yamaguchi, H., 1993, "Investigation on Propeller performance in Uniform and Blocked Flow for the Lifting Surface Calculations", Report NRC LM-1993-11, National Research Council of Canada, St.John's.

Zou, B., 1996, "Ships in ice: The interaction process and principles of design", Ph.D Thesis, Memorial University of Newfoundland.